

Algorithmic recourse under imperfect causal knowledge: a probabilistic approach

Amir-Hossein Karimi^{*1,2} Julius von Kügelgen^{*1,3} Bernhard Schölkopf¹ Isabel Valera^{1,4}

¹Max Planck Institute for Intelligent Systems, Tübingen, Germany

²Max Planck ETH Center for Learning Systems, Zürich, Switzerland

³Department of Engineering, University of Cambridge, United Kingdom

⁴Department of Computer Science, Saarland University, Saarbrücken, Germany
{amir, jvk, bs, ivalera}@tue.mpg.de

Abstract

Recent work has discussed the limitations of counterfactual explanations to recommend actions for algorithmic recourse, and argued for the need of taking causal relationships between features into consideration. Unfortunately, in practice, the true underlying structural causal model is generally unknown. In this work, we first show that it is impossible to guarantee recourse without access to the true structural equations. To address this limitation, we propose two probabilistic approaches to select optimal actions that achieve recourse with high probability given limited causal knowledge (e.g., only the causal graph). The first captures uncertainty over structural equations under additive Gaussian noise, and uses Bayesian model averaging to estimate the counterfactual distribution. The second removes any assumptions on the structural equations by instead computing the average effect of recourse actions on individuals similar to the person who seeks recourse, leading to a novel subpopulation-based interventional notion of recourse. We then derive a gradient-based procedure for selecting optimal recourse actions, and empirically show that the proposed approaches lead to more reliable recommendations under imperfect causal knowledge than non-probabilistic baselines.

1 Introduction

As machine learning algorithms are increasingly used to assist consequential decision making in a wide range of real world settings [28, 33], providing explanations for the decision of these black-box models becomes crucial [5, 46]. A popular approach is that of (nearest) *counterfactual explanations*, which refer to the closest feature instantiations that would have resulted in a changed prediction [47]. While providing some insight (explanation) into the underlying black-box classifier, such counterfactual explanations do not directly translate into actionable recommendations to individuals for obtaining a more favourable prediction—a related task referred to as *algorithmic recourse* [44]. Importantly, prior work on both counterfactual explanations and algorithmic recourse treats features as independently manipulable inputs, thus *ignoring the causal relationships between features*.

In this context, recent work [17] has argued for the need of taking into account the causal structure between features to find a set of actions (in the form of interventions) that guarantees recourse. However, while this approach is theoretically sound, it involves computing counterfactuals in the *true underlying structural causal model* (SCM) [27], and thus relies on strong impractical assumptions. Specifically, it requires complete knowledge of the true structural equations. While for many applica-

^{*}Equal contribution

tions it is possible to draw a causal diagram from expert knowledge, assumptions about the form of structural equations are, in general, not testable and may thus not hold in practice [30]. As a result, counterfactuals computed using a misspecified causal model may be inaccurate and recommend actions that are sub-optimal or, even worse, ineffective to achieve recourse.

In this work, we focus on the problem of algorithmic recourse when only *limited causal knowledge* is available (as it is generally the case). To this end, we propose two probabilistic approaches, which allows us to relax the strong assumptions in [17]. In the first approach, we assume that, while the underlying SCM is unknown, it belongs to the family of additive Gaussian noise models [12, 29]. Under this assumption, we make use of Gaussian processes (GPs) [50] to average predictions over a whole family of SCMs, and thus to obtain a distribution over counterfactual outcomes, which forms the basis for *individualised algorithmic recourse*. In the second approach, we further relax our assumptions by removing any assumptions on the form of the structural equations, and instead consider *subpopulation-based algorithmic recourse*, by estimating the effect of interventions for individuals similar to the one for which we aim to achieve recourse. This approach is based on the idea of the conditional average treatment effect (CATE) [1], and relies on conditional variational autoencoders (CVAEs) [39] to estimate the interventional distribution. In both cases, we assume that the causal graph is known or can be postulated from expert knowledge, as without such an assumption causal reasoning from observational data is not possible [30, Prop. 4.1].

In more detail, we first demonstrate as a motivating negative result that recourse guarantees are only possible if the true SCM is known (§3). Then, we introduce two probabilistic approaches for handling different levels of uncertainty in the structural equations (§4 and §5), and propose a gradient-based method to find a set of actions that achieves recourse with a given probability at minimum cost (§6). Our experiments (§7) on synthetic and semi-synthetic loan approval data, show the need for probabilistic approaches to achieve algorithmic recourse in practice, as point estimates of the underlying true SCM often propose invalid recommendations or achieve recourse only at higher cost. Importantly, our results also show that subpopulation-based recourse is the right approach to adopt when assumptions such as additive noise do not hold. A user-friendly implementation of all methods that only requires specification of the causal graph and a training set is included in the supplement.

2 Background and related work

Causality: structural causal models, interventions, and counterfactuals. To reason formally about causal relations between features $\mathbf{X} = \{X_1, \dots, X_d\}$, we adopt the *structural causal model* (SCM) framework [27].² Specifically, we assume that the data-generating process of \mathbf{X} is described by an (unknown) underlying SCM \mathcal{M} of the general form

$$\mathcal{M} = (\mathbf{S}, P_{\mathbf{U}}), \quad \mathbf{S} = \{X_r := f_r(\mathbf{X}_{\text{pa}(r)}, U_r)\}_{r=1}^d, \quad P_{\mathbf{U}} = P_{U_1} \times \dots \times P_{U_d}, \quad (1)$$

where the structural equations \mathbf{S} are a set of assignments generating each observed variable X_r as a deterministic function f_r of its causal parents $\mathbf{X}_{\text{pa}(r)} \subseteq \mathbf{X} \setminus X_r$ and an unobserved noise variable U_r . The assumption of mutually independent noises (i.e., a fully factorised $P_{\mathbf{U}}$) entails that there is no hidden confounding and is referred to as *causal sufficiency*. An SCM is often illustrated by its associated causal graph \mathcal{G} , which is obtained by drawing a directed edge from each node in $\mathbf{X}_{\text{pa}(r)}$ to X_r for $r \in [d] := \{1, \dots, d\}$, see Fig. 1b and 1c for an example. We assume throughout that \mathcal{G} is acyclic. In this case, \mathcal{M} implies a unique observational distribution $P_{\mathbf{X}}$, which factorises over \mathcal{G} , defined as the push-forward of $P_{\mathbf{U}}$ via \mathbf{S} .³

Importantly, the SCM framework also entails *interventional distributions* describing a situation in which some variables are manipulated externally. E.g., using the *do*-operator, an intervention which fixes $\mathbf{X}_{\mathcal{I}}$ to θ (where $\mathcal{I} \subseteq [d]$) is denoted by $\text{do}(\mathbf{X}_{\mathcal{I}} = \theta)$. The corresponding distribution of the remaining variables $\mathbf{X}_{-\mathcal{I}}$ can be computed by replacing the structural equations for $\mathbf{X}_{\mathcal{I}}$ in \mathbf{S} to obtain the new set of equations $\mathbf{S}^{\text{do}(\mathbf{X}_{\mathcal{I}} = \theta)}$. The interventional distribution $P_{\mathbf{X}_{-\mathcal{I}}|\text{do}(\mathbf{X}_{\mathcal{I}} = \theta)}$ is then given by the observational distribution implied by the manipulated SCM $(\mathbf{S}^{\text{do}(\mathbf{X}_{\mathcal{I}} = \theta)}, P_{\mathbf{U}})$.

Similarly, an SCM also implies distributions over *counterfactuals*—statements about a world in which a hypothetical intervention was performed *all else being equal*. For example, *given* observation \mathbf{x}^{F} we

²Also known as non-parametric structural equation model with independent errors (NPSEM-IE).

³I.e., for $r \in [d]$, $P_{X_r|\mathbf{X}_{\text{pa}(r)}}(X_r|\mathbf{X}_{\text{pa}(r)}) := P_{U_r}(f_r^{-1}(X_r|\mathbf{X}_{\text{pa}(r)}))$, where $f_r^{-1}(X_r|\mathbf{X}_{\text{pa}(r)})$ denotes the pre-image of X_r given $\mathbf{X}_{\text{pa}(r)}$ under f_r , i.e., $f_r^{-1}(X_r|\mathbf{X}_{\text{pa}(r)}) := \{u \in \mathcal{U}_r : f_r(\mathbf{X}_{\text{pa}(r)}, u) = X_r\}$.

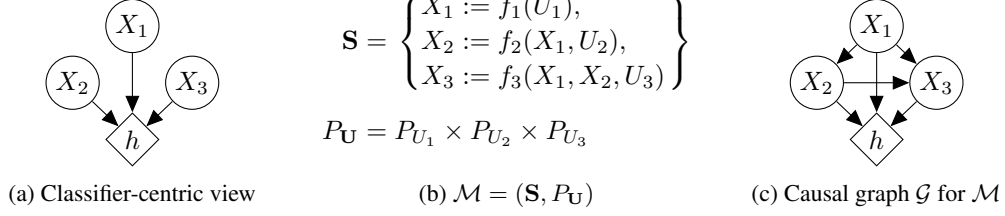


Figure 1: A view commonly adopted for counterfactual explanations (a) treats features as independently manipulable inputs to a given fixed and deterministic classifier h . In the causal approach to algorithmic recourse taken in this work, we instead view variables as causally related to each other by a structural causal model (SCM) \mathcal{M} (b) with associated causal graph \mathcal{G} (c).

can ask what would have happened if $\mathbf{X}_{\mathcal{I}}$ had instead taken the value θ . We denote the counterfactual variable by $\mathbf{X}(do(\mathbf{X}_{\mathcal{I}} = \theta))|\mathbf{x}^F$, whose distribution can be computed in three steps [27]:

1. *Abduction*: compute the posterior distribution over background variables given \mathbf{x}^F , $P_{\mathbf{U}|\mathbf{x}^F}$;
2. *Action*: perform the intervention to obtain the new structural equations $\mathbf{S}^{do(\mathbf{X}_{\mathcal{I}} = \theta)}$; and,
3. *Prediction*: $P_{\mathbf{X}(do(\mathbf{X}_{\mathcal{I}} = \theta))|\mathbf{x}^F}$ is the distribution induced by the resulting SCM $(\mathbf{S}^{do(\mathbf{X}_{\mathcal{I}} = \theta)}, P_{\mathbf{U}|\mathbf{x}^F})$.

Explainable ML: “counterfactual” explanations and (causal) algorithmic recourse. Assume that we are given a binary probabilistic classifier $h : \mathcal{X} \rightarrow [0, 1]$ trained to make decisions about i.i.d. samples from the data distribution $P_{\mathbf{X}}$.⁴ For ease of illustration, we adopt the setting of loan approval as a running example, i.e., $h(\mathbf{x}) \geq 0.5$ denotes that a loan is granted and $h(\mathbf{x}) < 0.5$ that it is denied. For a given individual \mathbf{x}^F that was denied a loan, $h(\mathbf{x}^F) < 0.5$, we aim to answer the following questions: “Why did individual \mathbf{x}^F not get the loan?” and “What would they have to change, preferably with minimal effort, to increase their chances for a future application?”.

A popular approach to this task is to find so-called (nearest) *counterfactual explanations* [47], where the term “counterfactual” is meant in the sense of the closest possible world with a different outcome [22]. Translating this idea to our setting, a counterfactual explanation \mathbf{x}^{CE} for an individual \mathbf{x}^F is given by a solution to the following optimisation problem:

$$\mathbf{x}^{CE} \in \arg \min_{\mathbf{x} \in \mathcal{X}} \text{dist}(\mathbf{x}, \mathbf{x}^F) \quad \text{subject to} \quad h(\mathbf{x}) \geq 0.5, \quad (2)$$

where $\text{dist}(\cdot, \cdot)$ is a similarity metric on \mathcal{X} , and additional constraints may be added to reflect plausibility, feasibility, or diversity of the obtained counterfactual explanations [15, 16, 24, 25, 31, 35].

Importantly, while \mathbf{x}^{CE} signifies the most similar individual to \mathbf{x}^F that would receive the loan, it does not inform \mathbf{x}^F on the actions they should perform to become \mathbf{x}^{CE} . To address this limitation, the recently proposed framework of *algorithmic recourse* focuses instead on the actions an individual can perform to achieve a more favourable outcome [44]. The emphasis is thus shifted from minimising a distance as in (2) to optimising a personalised cost function $\text{cost}^F(\cdot)$ over a set of actions \mathbb{A}^F which individual \mathbf{x}^F can perform. However, most prior work on both counterfactual explanations and algorithmic recourse considers features as independently manipulable inputs to the classifier h (see Fig. 1a), and therefore, ignores the potentially rich causal structure over \mathbf{X} (see Fig. 1c).

In the most relevant work to the current [17], the authors approach the algorithmic recourse problem from a causal perspective within the SCM framework (see §2) and propose to view recourse actions $a \in \mathbb{A}^F$ as interventions of the form $do(\mathbf{X}_{\mathcal{I}} = \theta)$. For the class of invertible SCMs, such as additive noise models (ANM) [12], where the structural equations \mathbf{S} are of the form

$$\mathbf{S} = \{X_r := f_r(\mathbf{X}_{\text{pa}(r)}) + U_r\}_{r=1}^d \implies u_r^F = x_r^F - f_r(\mathbf{x}_{\text{pa}(r)}^F), \quad r \in [d], \quad (3)$$

they propose to use the three steps of structural counterfactuals in [27] to assign a single counterfactual $\mathbf{x}^{\text{SCF}}(a) := \mathbf{x}(a)|\mathbf{x}^F$ to each action $a = do(\mathbf{X}_{\mathcal{I}} = \theta) \in \mathbb{A}^F$, and solve the optimisation problem,

$$a^F = \arg \min_{a = do(\mathbf{X}_{\mathcal{I}} = \theta) \in \mathbb{A}^F} \text{cost}^F(a) \quad \text{subject to} \quad h(\mathbf{x}^{\text{SCF}}(a)) \geq 0.5. \quad (4)$$

⁴Following the related literature, we consider a binary classification task by convention; most of our considerations extend to multi-class classification or regression settings as well though.

3 Negative result: no recourse guarantees for unknown structural equations

The main limitation of [17], or equivalently the approach in (4), is that the true underlying causal model \mathcal{M}_\star (including the structural equations \mathbf{S}_\star) is assumed to be known, which is in general not the case. In practice, the structural counterfactual $\mathbf{x}^{\text{SCF}}(a)$ can only be computed using an approximate (and likely imperfect) SCM $\mathcal{M} = (\mathbf{S}, P_U)$, which is estimated from data assuming a particular form of the structural equation as in (3). However, assumptions on the form of \mathbf{S}_\star are generally untestable—not even with a randomised experiment—since there exist multiple SCMs which imply the same observational and interventional distributions, but entail different structural counterfactuals.

Example 1 (adapted from 6.19 in [30]). *Consider the following two SCMs \mathcal{M}_A and \mathcal{M}_B which arise from the general form in Figure 1b by choosing $U_1, U_2 \sim \text{Bernoulli}(0.5)$ and $U_3 \sim \text{Uniform}(\{0, \dots, K\})$ independently in both \mathcal{M}_A and \mathcal{M}_B , with structural equations*

$$\begin{aligned} X_1 &:= U_1, & \text{in } \{\mathcal{M}_A, \mathcal{M}_B\}, \\ X_2 &:= X_1(1 - U_2), & \text{in } \{\mathcal{M}_A, \mathcal{M}_B\}, \\ X_3 &:= \mathbb{I}_{X_1 \neq X_2}(\mathbb{I}_{U_3 > 0}X_1 + \mathbb{I}_{U_3 = 0}X_2) + \mathbb{I}_{X_1 = X_2}U_3, & \text{in } \mathcal{M}_A, \\ X_3 &:= \mathbb{I}_{X_1 \neq X_2}(\mathbb{I}_{U_3 > 0}X_1 + \mathbb{I}_{U_3 = 0}X_2) + \mathbb{I}_{X_1 = X_2}(K - U_3), & \text{in } \mathcal{M}_B. \end{aligned}$$

Then \mathcal{M}_A and \mathcal{M}_B both imply exactly the same observational and interventional distributions, and thus are indistinguishable from empirical data. However, having observed $\mathbf{x}^F = (1, 0, 0)$, they predict different counterfactuals had X_1 been 0, i.e., $\mathbf{x}^{\text{SCF}}(X_1 = 0) = (0, 0, 0)$ and $(0, 0, K)$, respectively.⁵

Confirming or refuting an assumed form of \mathbf{S}_\star would thus require counterfactual data which is, by definition, never available. Thus, example 1 proves the following proposition by contradiction.

Proposition 1 (Lack of recourse guarantees). *Algorithmic recourse can, in general, be guaranteed only if the true structural equations are known, irrespective of the amount and type of available data.*

Remark 1. *The converse of Proposition 1 does not hold. E.g., given $\mathbf{x}^F = (1, 0, 1)$ in Example 1, abduction in either model yields $U_3 > 0$, so the counterfactual of X_3 cannot be predicted exactly.*

Building on the framework in [17], we next present two novel approaches for causal algorithmic recourse under unknown structural equations. The first approach in §4 aims to estimate the counterfactual distribution under the assumption of ANMs (3) with Gaussian noise for the structural equations. The second approach in §5 makes no assumptions about the structural equations, and instead of approximating the structural equations, it considers the effect of interventions on a sub-population similar to \mathbf{x}^F . We recall that the causal graph is assumed to be known throughout.

4 Individualised algorithmic recourse via (probabilistic) counterfactuals

Since the true SCM \mathcal{M}_\star is unknown, one approach to solving (4) is to learn an approximate SCM \mathcal{M} within a given model class from training data $\{\mathbf{x}^i\}_{i=1}^n$. For example, for an ANM (3) with zero-mean noise, the functions f_r can be learned via linear or kernel (ridge) regression of X_r given $\mathbf{X}_{\text{pa}(r)}$ as input. We refer to these approaches as \mathcal{M}_{LIN} and \mathcal{M}_{KR} , respectively. \mathcal{M} can then be used in place of \mathcal{M}_\star to infer the noise values as in (3), and subsequently to predict a *single-point counterfactual* $\mathbf{x}^{\text{SCF}}(a)$ to be used in (4). However, the learned causal model \mathcal{M} may be imperfect, and thus lead to wrong counterfactuals due to, e.g., the finite sample of the observed data, or more importantly, due to model misspecification (i.e., assuming a wrong parametric form for the structural equations).

To solve such limitation, we adopt a Bayesian approach to account for the uncertainty in the estimation of the structural equations. Specifically, we assume additive Gaussian noise and rely on probabilistic regression using a Gaussian process (GP) prior over the functions f_r [50].

Definition 1 (GP-SCM). *A Gaussian process SCM (GP-SCM) over \mathbf{X} refers to the model*

$$X_r := f_r(\mathbf{X}_{\text{pa}(r)}) + U_r, \quad f_r \sim \mathcal{GP}(0, k_r), \quad U_r \sim \mathcal{N}(0, \sigma_r^2), \quad r \in [d], \quad (5)$$

with covariance functions $k_r : \mathcal{X}_{\text{pa}(r)} \times \mathcal{X}_{\text{pa}(r)} \rightarrow \mathbb{R}$, e.g., RBF kernels for continuous $X_{\text{pa}(r)}$.

While GPs have previously been studied in a causal context for structure learning [10, 45], estimating treatment effects [2, 34], or learning SCMs with latent variables and measurement error [38], our goal

⁵This follows from abduction on $\mathbf{x}^F = (1, 0, 0)$ which for both \mathcal{M}_A and \mathcal{M}_B implies $U_3 = 0$.

here is to account for the uncertainty over f_r in the computation of the posterior over U_r , and thus to obtain a *counterfactual distribution*, as summarised in the following propositions.

Proposition 2 (GP-SCM noise posterior). *Let $\{\mathbf{x}^i\}_{i=1}^n$ be an observational sample from (5). For each $r \in [d]$ with non empty parent set $|pa(r)| > 0$, the posterior distribution of the noise vector $\mathbf{u}_r = (u_r^1, \dots, u_r^n)$, conditioned on $\mathbf{x}_r = (x_r^1, \dots, x_r^n)$ and $\mathbf{X}_{pa(r)} = (\mathbf{x}_{pa(r)}^1, \dots, \mathbf{x}_{pa(r)}^n)$, is given by*

$$\mathbf{u}_r | \mathbf{X}_{pa(r)}, \mathbf{x}_r \sim \mathcal{N}(\sigma_r^2(\mathbf{K} + \sigma_r^2 \mathbf{I})^{-1} \mathbf{x}_r, \sigma_r^2(\mathbf{I} - \sigma_r^2(\mathbf{K} + \sigma_r^2 \mathbf{I})^{-1})), \quad (6)$$

where $\mathbf{K} := (k_r(\mathbf{x}_{pa(r)}^i, \mathbf{x}_{pa(r)}^j))_{ij}$ denotes the Gram matrix.

Next, in order to compute counterfactual distributions, we rely on ancestral sampling (according to the causal graph) of the descendants of the intervention targets $\mathbf{X}_{\mathcal{I}}$ using the noise posterior of (6). The counterfactual distribution of each descendant X_r is given by the following proposition.

Proposition 3 (GP-SCM counterfactual distribution). *Let $\{\mathbf{x}^i\}_{i=1}^n$ be an observational sample from (5). Then, for $r \in [d]$ with $|pa(r)| > 0$, the counterfactual distribution over X_r had $\mathbf{X}_{pa(r)}$ been $\tilde{\mathbf{x}}_{pa(r)}^F$ (instead of $\mathbf{x}_{pa(r)}^F$) for individual $\mathbf{x}^F \in \{\mathbf{x}^i\}_{i=1}^n$ is given by*

$$X_r(\mathbf{X}_{pa(r)} = \tilde{\mathbf{x}}_{pa(r)}) | \mathbf{x}^F, \{\mathbf{x}^i\}_{i=1}^n \sim \mathcal{N}(\mu_r^F + \tilde{\mathbf{k}}^T(\mathbf{K} + \sigma_r^2 \mathbf{I})^{-1} \mathbf{x}_r, s_r^F + \tilde{k} - \tilde{\mathbf{k}}^T(\mathbf{K} + \sigma_r^2 \mathbf{I})^{-1} \tilde{\mathbf{k}}), \quad (7)$$

where $\tilde{k} := k_r(\tilde{\mathbf{x}}_{pa(r)}, \tilde{\mathbf{x}}_{pa(r)})$, $\tilde{\mathbf{k}} := (k_r(\tilde{\mathbf{x}}_{pa(r)}, \mathbf{x}_{pa(r)}^1), \dots, k_r(\tilde{\mathbf{x}}_{pa(r)}, \mathbf{x}_{pa(r)}^n))$, \mathbf{x}_r and \mathbf{K} as defined in Proposition 2, and μ_r^F and s_r^F are the posterior mean and variance of u_r^F given by (6).

All proofs can be found in Appendix A. We can now generalise the recourse problem (4) to our probabilistic setting by replacing the single-point counterfactual $\mathbf{x}^{\text{SCF}}(a)$ with the counterfactual random variable $\mathbf{X}^{\text{SCF}}(a) := \mathbf{X}(a) | \mathbf{x}^F$. As a consequence, it no longer makes sense to consider a hard constraint of the form $h(\mathbf{x}^{\text{SCF}}(a)) > 0.5$, i.e., that the prediction needs to change. Instead, we can reason about the expected classifier output under the counterfactual distribution, leading to the following *probabilistic version of the individualised recourse optimisation problem*:

$$\min_{a = do(\mathbf{X}_{\mathcal{I}} = \boldsymbol{\theta}) \in \mathbb{A}^F} \text{cost}^F(a) \quad \text{subject to} \quad \mathbb{E}_{\mathbf{X}^{\text{SCF}}(a)} [h(\mathbf{X}^{\text{SCF}}(a))] \geq \text{thresh}(a). \quad (8)$$

Note that the threshold $\text{thresh}(a)$ is allowed to depend on a . For example, an intuitive choice is

$$\text{thresh}(a) = 0.5 + \gamma_{\text{LCB}} \sqrt{\text{Var}_{\mathbf{X}^{\text{SCF}}(a)} [h(\mathbf{X}^{\text{SCF}}(a))]} \quad (9)$$

which has the interpretation of the lower-confidence bound crossing the decision boundary of 0.5. Note that larger values of the hyperparameter γ_{LCB} lead to a more conservative approach to recourse, while for $\gamma_{\text{LCB}} = 0$ merely crossing the decision boundary with $\geq 50\%$ chance suffices.

5 Subpopulation-based algorithmic recourse via interventions and CATES

The GP-SCM approach in §4 allows us to average over an infinite number of (non-)linear structural equations, under the assumption of additive Gaussian noise. However, this assumption may still not hold under the true SCM, leading to sub-optimal or inefficient solutions to the recourse problem. Next, we remove any assumptions about the structural equations, and propose a second approach that does not aim to approximate an individualised counterfactual distribution, but instead considers the effect of interventions on a subpopulation defined by certain shared characteristics with the given (factual) individual \mathbf{x}^F . The key idea behind this approach resembles the notion of conditional average treatment effects (CATE) [1] (illustrated in Fig. 2a) and is based on the fact that any intervention $do(\mathbf{X}_{\mathcal{I}} = \boldsymbol{\theta})$ only influences the descendants $d(\mathcal{I})$ of the intervened-upon variables, while the non-descendants $nd(\mathcal{I})$ remain unaffected. Thus, when evaluating an intervention, we can condition on $\mathbf{X}_{nd(\mathcal{I})} = \mathbf{x}_{nd(\mathcal{I})}^F$, thus selecting a subpopulation of individuals similar to the factual subject.

Specifically, we propose to solve the following *subpopulation-based recourse optimisation problem*

$$\min_{a \in \mathbb{A}^F} \text{cost}^F(a) \quad \text{subject to} \quad \mathbb{E}_{\mathbf{X}_{d(\mathcal{I})} | do(\mathbf{X}_{\mathcal{I}} = \boldsymbol{\theta}), \mathbf{x}_{nd(\mathcal{I})}^F} [h(\mathbf{x}_{nd(\mathcal{I})}^F, \boldsymbol{\theta}, \mathbf{X}_{d(\mathcal{I})})] \geq \text{thresh}(a), \quad (10)$$

where, in contrast to (8), the expectation is taken over the corresponding interventional distribution.

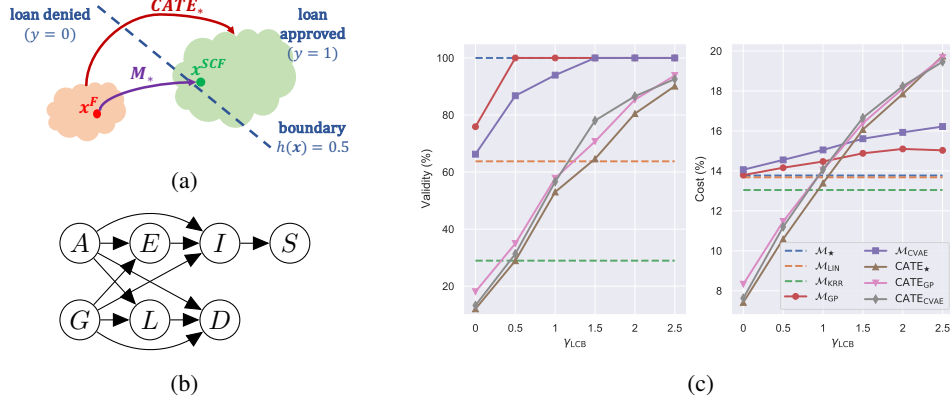


Figure 2: (a) Illustration of point- and subpopulation-based recourse approaches. (b) Assumed causal graph for the semi-synthetic loan approval dataset. (c) Trade-off between validity and cost which can be controlled via γ_{LCB} for the probabilistic recourse methods.

In general, this interventional distribution does not match the conditional distribution, i.e., $P_{\mathbf{X}_{d(I)}|do(\mathbf{X}_I=\theta), \mathbf{x}_{nd(I)}^F} \neq P_{\mathbf{X}_{d(I)}|\mathbf{X}_I=\theta, \mathbf{x}_{nd(I)}^F}$, because some spurious correlations in the observational distribution do not transfer to the interventional setting. For example, in Fig. 1c we have that $P_{X_2|do(X_1=x_1, X_3=x_3)} = P_{X_2|X_1=x_1} \neq P_{X_2|X_1=x_1, X_3=x_3}$. Fortunately, the interventional distribution can still be identified from the observational one, as stated in the following proposition.

Proposition 4. *Subject to causal sufficiency, $P_{\mathbf{X}_{d(I)}|do(\mathbf{X}_I=\theta), \mathbf{x}_{nd(I)}^F}$ is observationally identifiable:*

$$p(\mathbf{X}_{d(I)}|do(\mathbf{X}_I=\theta), \mathbf{x}_{nd(I)}^F) = \prod_{r \in d(I)} p(X_r|\mathbf{X}_{pa(r)}) \Big|_{\mathbf{X}_I=\theta, \mathbf{X}_{nd(I)}=\mathbf{x}_{nd(I)}^F}. \quad (11)$$

As evident from Proposition 4, tackling the optimisation problem in (10) in the general case (i.e., for arbitrary graphs and intervention sets \mathcal{I}) requires estimating the stable conditionals $P_{X_r|\mathbf{X}_{pa(r)}}$ (a.k.a. causal Markov kernels) in order to compute the interventional expectation via (11). For convenience (see §6 for details), here we opt for latent-variable implicit density models, but other conditional density estimation approaches may also be used [e.g., 4, 6, 43]. Specifically, we model each conditional $p(x_r|\mathbf{x}_{pa(r)})$ with a conditional variational autoencoder (CVAE) [39] as:

$$p(x_r|\mathbf{x}_{pa(r)}) \approx p_{\psi_r}(x_r|\mathbf{x}_{pa(r)}) = \int p_{\psi_r}(x_r|\mathbf{x}_{pa(r)}, \mathbf{z}_r) p(\mathbf{z}_r) d\mathbf{z}_r, \quad p(\mathbf{z}_r) := \mathcal{N}(\mathbf{0}, \mathbf{I}). \quad (12)$$

To facilitate sampling x_r (and in analogy to the deterministic mechanisms f_r in SCMs), we opt for deterministic decoders in the form of neural nets D_r parametrised by ψ_r , i.e., $p_{\psi_r}(x_r|\mathbf{x}_{pa(r)}, \mathbf{z}_r) := \delta(x_r - D_r(\mathbf{x}_{pa(r)}, \mathbf{z}_r; \psi_r))$, and rely on variational inference [48], amortised with approximate posteriors $q_{\phi_r}(\mathbf{z}_r|x_r, \mathbf{x}_{pa(r)})$ parametrised by encoders in the form of neural nets with parameters ϕ_r . We learn both the encoder and decoder parameters by maximising the evidence lower bound (ELBO) using stochastic gradient descent [7, 19, 20, 32]. For further details, we refer to Appendix B.

Remark 2. *The collection of CVAEs can be interpreted as learning an approximate SCM of the form*

$$\mathcal{M}_{CVAE} : \quad \mathbf{S} = \{X_r := D_r(\mathbf{X}_{pa(r)}, \mathbf{z}_r; \psi_r)\}_{r=1}^d, \quad \mathbf{z}_r \sim \mathcal{N}(\mathbf{0}, \mathbf{I}) \quad \forall r \in [d] \quad (13)$$

However, this family of SCMs may not allow to identify the true SCM (provided it can be expressed as above) from data without additional assumptions. Moreover, exact posterior inference over \mathbf{z}_r given \mathbf{x}^F is intractable, and we need to resort to approximations instead. It is thus unclear whether sampling from $q_{\phi_r}(\mathbf{z}_r|x_r^F, \mathbf{x}_{pa(r)}^F)$ instead of from $p(\mathbf{z}_r)$ in (12) can be interpreted as a counterfactual within (13). For further discussion on such “pseudo-counterfactuals” we refer to Appendix C.

6 Solving the probabilistic-recourse optimisation problems

We now discuss how to solve the resulting optimisation problems in (8) and (10). First, note that both problems differ only on the distribution over which the expectation in the constraint is taken: in (8)

Table 1: Experimental results for the gradient-based approach on different 3-variable SCMs. We show average performance for $N_{\text{runs}} = 50$, $N_{\text{MC-samples}} = 100$, and $\gamma_{\text{LCB}} = 2$.

Method	LINEAR SCM			NON-LINEAR ANM			NON-ADDITIVE SCM		
	Valid _* (%)	LCB	Cost (%)	Valid _* (%)	LCB	Cost (%)	Valid _* (%)	LCB	Cost (%)
\mathcal{M}_\star	100	-	7.5±4.1	100	-	21.2±11.4	100	-	6.3±3.5
\mathcal{M}_{LIN}	100	-	7.8±4.2	52	-	20.1± 6.9	94	-	6.3±3.5
\mathcal{M}_{KR}	100	-	7.8±4.1	98	-	21.4±11.4	90	-	6.2±3.5
\mathcal{M}_{GP}	100	.54±.03	9.0±4.1	100	.55±.03	23.0±11.7	100	.54±.03	6.2±3.5
$\mathcal{M}_{\text{CVAE}}$	100	.53±.02	9.0±4.2	96	.54±.04	24.2±10.0	96	.54±.03	6.2±3.5
CATE _*	96	.54±.04	9.5±4.2	92	.55±.04	24.7±12.2	98	.54±.03	6.2±3.6
CATE _{GP}	94	.54±.04	9.5±4.2	96	.56±.05	25.3±11.8	92	.53±.03	6.2±3.6
CATE _{CVAE}	94	.54±.05	9.6±4.3	98	.53±.03	26.3±11.1	94	.53±.02	6.2±3.6

this is the counterfactual distribution of the descendants given in Proposition 3; and in (10) it is the interventional distribution identified in Proposition 4. In either case, computing the expectation for an arbitrary classifier h is intractable. Here, we approximate these integrals via Monte Carlo by sampling $\mathbf{x}_{\text{d}(\mathcal{I})}^{(m)}$ from the interventional or counterfactual distributions resulting from $a = \text{do}(\mathbf{X}_{\mathcal{I}} = \boldsymbol{\theta})$, i.e.,

$$\mathbb{E}_{\mathbf{X}_{\text{d}(\mathcal{I})}|\boldsymbol{\theta}}[h(\mathbf{x}_{\text{nd}(\mathcal{I})}^{\text{F}}, \boldsymbol{\theta}, \mathbf{X}_{\text{d}(\mathcal{I})})] \approx \frac{1}{M} \sum_{m=1}^M h(\mathbf{x}_{\text{nd}(\mathcal{I})}^{\text{F}}, \boldsymbol{\theta}, \mathbf{x}_{\text{d}(\mathcal{I})}^{(m)}).$$

Brute-force approach. A way to solve (8) and (10) is to (i) iterate over $a \in \mathbb{A}^{\text{F}}$, with \mathbb{A}^{F} being a finite set of feasible actions (possibly as a result of discretising in the case of a continuous search space); (ii) approximately evaluate the constraint via Monte Carlo; and (iii) select a minimum cost action amongst all evaluated candidates satisfying the constraint. However, this may be computationally prohibitive and yield suboptimal interventions due to discretisation.

Gradient-based approach. Recall that, for actions of the form $a = \text{do}(\mathbf{X}_{\mathcal{I}} = \boldsymbol{\theta})$, we need to optimise over both the intervention *targets* \mathcal{I} and the intervention *values* $\boldsymbol{\theta}$. Selecting targets is a hard combinatorial optimisation problem, as there are $2^{d'}$ possible choices for $d' \leq d$ actionable features, with a potentially infinite number of intervention values. We therefore consider different choices of targets \mathcal{I} in parallel, and propose a gradient-based approach suitable for differentiable classifiers to efficiently find an optimal $\boldsymbol{\theta}$ for a given intervention set \mathcal{I} .⁶ In particular, we first rewrite the constrained optimisation problem in unconstrained form with Lagrangian [18, 21]:

$$\mathcal{L}(\boldsymbol{\theta}, \lambda) := \text{cost}^{\text{F}}(a) + \lambda(\text{thresh}(a) - \mathbb{E}_{\mathbf{X}_{\text{d}(\mathcal{I})}|\boldsymbol{\theta}}[h(\mathbf{x}_{\text{nd}(\mathcal{I})}^{\text{F}}, \boldsymbol{\theta}, \mathbf{X}_{\text{d}(\mathcal{I})})]). \quad (14)$$

We then solve the saddle point problem $\min_{\boldsymbol{\theta}} \max_{\lambda} \mathcal{L}(\boldsymbol{\theta}, \lambda)$ arising from (14) with stochastic gradient descent [7, 19]. Since both the GP-SCM counterfactual (7) and the CVAE interventional distributions (12) admit a reparametrisation trick [20, 32], we can differentiate through the constraint:

$$\nabla_{\boldsymbol{\theta}} \mathbb{E}_{\mathbf{X}_{\text{d}(\mathcal{I})}}[h(\mathbf{x}_{\text{nd}(\mathcal{I})}^{\text{F}}, \boldsymbol{\theta}, \mathbf{X}_{\text{d}(\mathcal{I})})] = \mathbb{E}_{\mathbf{z} \sim \mathcal{N}(\mathbf{0}, \mathbf{I})}[\nabla_{\boldsymbol{\theta}} h(\mathbf{x}_{\text{nd}(\mathcal{I})}^{\text{F}}, \boldsymbol{\theta}, \mathbf{x}_{\text{d}(\mathcal{I})}(\mathbf{z}))]. \quad (15)$$

Here, $\mathbf{x}_{\text{d}(\mathcal{I})}(\mathbf{z})$ is obtained by iteratively computing all descendants in topological order: either substituting \mathbf{z} together with the other parents into the decoders D_r for the CVAEs, or by using the Gaussian reparametrisation $x_r(\mathbf{z}) = \mu + \sigma \mathbf{z}$ with μ and σ given by (7) for the GP-SCM. A similar gradient estimator for the variance which enters $\text{thresh}(a)$ for $\gamma_{\text{LCB}} \neq 0$ is derived in Appendix F.

7 Experimental results

In our experiments, we compare the naive point-based recourse approaches \mathcal{M}_{LIN} and \mathcal{M}_{KR} mentioned at the beginning of §4; the counterfactual GP-SCM \mathcal{M}_{GP} ; and the CVAE approach for sub-population-based recourse (CATE_{CVAE}). For completeness, we also consider a CATE_{GP} approach as a GP can also be seen as modelling each conditional as a Gaussian,⁷ and also evaluate the “pseudo-counterfactual” $\mathcal{M}_{\text{CVAE}}$ approach discussed in Remark 2. Finally, we report oracle performance for individualised \mathcal{M}_\star and sub-population-based recourse methods CATE_{*} by sampling counterfactuals and interventions from the true underlying SCM. Additional results are provided in Appendix E.

⁶For large d when enumerating all \mathcal{I} becomes computationally prohibitive, we can upper-bound the allowed number of variables to be intervened on simultaneously (e.g., $|\mathcal{I}| \leq 3$), or choose a greedy approach to select \mathcal{I} .

⁷Sampling from the noise prior instead of the posterior in (6) leads to an interventional distribution in (7).

Table 2: Experimental results for the 7-variable SCM for loan-approval. We show average performance for $N_{\text{runs}} = 50+$, $N_{\text{MC-samples}} = 100$, and $\gamma_{\text{LCB}} = 2.5$. For linear and non-linear logistic regression as classifiers, we use the gradient-based approach, whereas for the non-differentiable random forest classifier we rely on the brute-force approach (with 10 discretised bins per dimension) to solve the recourse optimisation problems.

Method	LINEAR LOG. REGR.			NON-LIN. LOG. REGR. (MLP)			RANDOM FOREST (BRUTE-FORCE)		
	Valid _* (%)	LCB	Cost (%)	Valid _* (%)	LCB	Cost (%)	Valid _* (%)	LCB	Cost (%)
\mathcal{M}_*	100	-	13.4±5.9	100	-	7.7±4.1	100	-	13.0±7.4
\mathcal{M}_{LIN}	64	-	13.3±5.9	88	-	7.7±4.0	93	-	13.3±7.5
\mathcal{M}_{KR}	29	-	12.7±5.4	67	-	7.6±4.0	88	-	13.1±7.4
\mathcal{M}_{GP}	100	.50±.00	15.0±5.9	100	.52±.02	8.7±4.5	100	.62±.11	15.1±7.6
$\mathcal{M}_{\text{CVAE}}$	100	.50±.00	16.2±6.2	100	.52±.03	9.0±4.8	100	.63±.11	15.4±7.6
CATE _*	90	.50±.03	19.7±6.6	93	.52±.03	9.1±5.3	90	.63±.12	16.0±6.7
CATE _{GP}	93	.50±.03	19.6±6.4	93	.51±.03	9.1±5.1	92	.63±.13	16.3±7.1
CATE _{CVAE}	92	.50±.03	19.4±6.0	95	.52±.03	9.2±5.1	93	.64±.12	16.4±7.1

Metrics. We compare recourse actions recommended by the different methods in terms of *cost*, computed as the L2-norm between the intervention θ and the factual value $\mathbf{x}_{\mathcal{I}}^F$, normalised by the range of each feature $r \in \mathcal{I}$ observed in the training data; and *validity*, computed as the percentage of individuals for which the recommended actions result in a favourable prediction under the true SCM). For our probabilistic recourse methods, we also report the lower confidence bound $\text{LCB} := \mathbb{E}[h] - \gamma_{\text{LCB}} \sqrt{\text{Var}[h]}$ of the selected action under the given method.

Synthetic 3-variable SCMs under different assumptions. In our first set of experiments, we consider three classes of SCMs over three variables with the same causal graph as in Fig. 1c. To test robustness of the different methods to assumptions about the form of the true structural equations, we consider a linear SCM, a non-linear ANM, and a more general SCM with non-additive noise. For further details on the exact form we refer to Appendix D.

Results are shown in Table 1. We observe that the point-based recourse approaches perform well in terms of both validity and cost, when their underlying assumptions are met. Otherwise, validity significantly drops as expected (see, e.g., the results of \mathcal{M}_{LIN} on the non-linear ANM, or of \mathcal{M}_{KR} on the non-additive SCM). In contrast, \mathcal{M}_{GP} achieves 100% validity for all datasets, albeit at slightly higher cost than the oracle \mathcal{M}_* . We observe that the CATE approaches all provide comparable results in terms of validity and cost, with the cost of the oracle CATE_{*} being the lowest. As expected, population-based approaches lead to higher cost than individual-based ones, since the latter only aims to achieve recourse at the individual level while the former does it at a subpopulation level (see Fig. 2a). Finally, while the “pseudo-counterfactual” $\mathcal{M}_{\text{CVAE}}$ gives reasonable results, it yields lower validity than its subpopulation counterpart CATE_{CVAE} for the non-linear ANM.

Semi-synthetic 7-variable SCM for loan-approval. We also test our methods on a larger semi-synthetic SCM inspired by the German Credit UCI dataset [26]. We consider the variables age A , gender G , education-level E , loan amount L , duration D , income I , and savings S with causal graph shown in Fig. 2b. We model age A , gender G and loan duration D as non-actionable variables, but consider D to be mutable, i.e., it cannot be manipulated directly but is allowed to change (e.g., as a consequence of an intervention on L). The SCM includes linear and non-linear relationships, as well as different types of variables and noise distributions, and is described in more detail in Appendix D.

The results are summarised in Table 2, where we observe that the insights discussed above similarly apply for data generated from a more complex SCM, and for different classifiers. Finally, we show the influence of γ_{LCB} on the performance of the proposed probabilistic approaches in Fig. 2c. We observe that lower values of γ_{LCB} lead to lower validity (and cost), especially for the CATE approaches. As γ_{LCB} increases validity approaches the corresponding oracles \mathcal{M}_* and CATE_{*}, outperforming the point-based recourse approaches. In summary, our probabilistic recourse approaches are not only more robust, but also allow controlling the trade-off between validity and cost using γ_{LCB} .

8 Discussion

In this work, we studied the problem of algorithmic recourse from a causal perspective. As negative result, we first showed that algorithmic recourse cannot be guaranteed in the absence of perfect knowledge about the underlying SCM governing the world, which unfortunately is not available in practice. To address this limitation, we proposed two probabilistic approaches to achieve recourse under more realistic assumptions. In particular, we derived i) an individual-level recourse approach based on GPs that approximates the counterfactual distribution by averaging over the family of additive Gaussian SCMs; and ii) a subpopulation-based approach, which assumes that only the causal graph is known and makes use of CVAES to estimate the conditional average treatment effect of an intervention on a subpopulation similar to the individual seeking recourse. Our experiments showed that the proposed probabilistic approaches not only result in more robust recourse interventions than approaches based on point estimates of the SCM, but also allows to trade-off validity and cost.

Throughout the paper, we have assumed a known causal graph and causal sufficiency. While this may not hold for all settings, it is the minimal necessary set of assumptions for causal reasoning from observational data alone. Access to instrumental variables or experimental data may help further relax these assumptions [3, 8, 40]. Moreover, if only a partial graph is available or some relations are known to be confounded, one will need to restrict recourse actions to the subset of interventions that are still identifiable [36, 37, 41]. An alternative approach could address causal sufficiency violations by relying on latent variable models to estimate confounders from multiple causes [49] or proxy variables [23]. We relegate the investigation of these settings to future work.

Acknowledgments and Disclosure of Funding

The authors would like to thank Adrian Weller, Floyd Kretschmar, Junhyung Park, Matthias Bauer, Miriam Rateike, Nicolo Ruggeri, Umang Bhatt, and Vidhi Lalchand for helpful feedback and discussions. Moreover, a special thanks to Adrià Garriga-Alonso for insightful input on some of the GP-derivations and to Adrián Javaloy Bornás for invaluable help with the CVAE-training.

References

- [1] Jason Abrevaya, Yu-Chin Hsu, and Robert P Lieli. Estimating conditional average treatment effects. *Journal of Business & Economic Statistics*, 33(4):485–505, 2015.
- [2] Ahmed M Alaa and Mihaela van der Schaar. Bayesian inference of individualized treatment effects using multi-task gaussian processes. In *Advances in Neural Information Processing Systems*, pages 3424–3432, 2017.
- [3] Joshua D Angrist, Guido W Imbens, and Donald B Rubin. Identification of causal effects using instrumental variables. *Journal of the American statistical Association*, 91(434):444–455, 1996.
- [4] David M Bashtannyk and Rob J Hyndman. Bandwidth selection for kernel conditional density estimation. *Computational Statistics & Data Analysis*, 36(3):279–298, 2001.
- [5] Umang Bhatt, Alice Xiang, Shubham Sharma, Adrian Weller, Ankur Taly, Yunhan Jia, Joydeep Ghosh, Ruchir Puri, José MF Moura, and Peter Eckersley. Explainable machine learning in deployment. In *Proceedings of the 2020 Conference on Fairness, Accountability, and Transparency*, pages 648–657, 2020.
- [6] Christopher M Bishop. Mixture density networks. 1994.
- [7] Léon Bottou and Olivier Bousquet. The tradeoffs of large scale learning. In *Advances in neural information processing systems*, pages 161–168, 2008.
- [8] Gregory F Cooper and Changwon Yoo. Causal discovery from a mixture of experimental and observational data. In *Proceedings of the Fifteenth conference on Uncertainty in artificial intelligence*, pages 116–125, 1999.
- [9] G. Darmon. Analyse des liaisons de probabilité. In *Proc. Int. Stat. Conferences 1947*, page 231, 1951.
- [10] Nir Friedman and Iftach Nachman. Gaussian process networks. In *Proceedings of the Sixteenth conference on Uncertainty in artificial intelligence*, pages 211–219, 2000.

- [11] Arthur Gretton, Karsten M Borgwardt, Malte J Rasch, Bernhard Schölkopf, and Alexander Smola. A kernel two-sample test. *Journal of Machine Learning Research*, 13(Mar):723–773, 2012.
- [12] Patrik O Hoyer, Dominik Janzing, Joris M Mooij, Jonas Peters, and Bernhard Schölkopf. Nonlinear causal discovery with additive noise models. In *Advances in neural information processing systems*, pages 689–696, 2009.
- [13] Aapo Hyvärinen and Petteri Pajunen. Nonlinear independent component analysis: Existence and uniqueness results. *Neural Networks*, 12(3):429–439, 1999.
- [14] Dominik Janzing and Bernhard Schölkopf. Causal inference using the algorithmic markov condition. *IEEE Transactions on Information Theory*, 56(10):5168–5194, 2010.
- [15] Shalmali Joshi, Oluwasanmi Koyejo, Warut Vijitbenjaronk, Been Kim, and Joydeep Ghosh. Towards realistic individual recourse and actionable explanations in black-box decision making systems. *arXiv preprint arXiv:1907.09615*, 2019.
- [16] Amir-Hossein Karimi, Gilles Barthe, Borja Belle, and Isabel Valera. Model-agnostic counterfactual explanations for consequential decisions. *arXiv preprint arXiv:1905.11190*, 2019.
- [17] Amir-Hossein Karimi, Bernhard Schölkopf, and Isabel Valera. Algorithmic recourse: from counterfactual explanations to interventions. *arXiv preprint arXiv:2002.06278*, 2020.
- [18] W. Karush. Minima of functions of several variables with inequalities as side conditions. *Master’s Thesis, Department of Mathematics, University of Chicago*, 1939.
- [19] Diederik P Kingma and Jimmy Ba. Adam: A method for stochastic optimization. In *3rd International Conference for Learning Representations*, 2015.
- [20] Diederik P Kingma and Max Welling. Auto-encoding variational Bayes. In *2nd International Conference on Learning Representations*, 2014.
- [21] Harold W Kuhn and Albert W Tucker. Nonlinear programming. In J. Neyman, editor, *Proceedings of the second Berkeley symposium on mathematical statistics and probability*. University of California Press, Berkeley, 1951.
- [22] David Lewis. *Counterfactuals*. Harvard University Press, 1973.
- [23] Christos Louizos, Uri Shalit, Joris M Mooij, David Sontag, Richard Zemel, and Max Welling. Causal effect inference with deep latent-variable models. In *Advances in Neural Information Processing Systems*, pages 6446–6456, 2017.
- [24] Divyat Mahajan, Chenhao Tan, and Amit Sharma. Preserving causal constraints in counterfactual explanations for machine learning classifiers. *arXiv preprint arXiv:1912.03277*, 2019.
- [25] Ramaravind K Mothilal, Amit Sharma, and Chenhao Tan. Explaining machine learning classifiers through diverse counterfactual explanations. In *Proceedings of the 2020 Conference on Fairness, Accountability, and Transparency*, pages 607–617, 2020.
- [26] Patrick M Murphy. UCI repository of machine learning databases. *ftp://pub/machine-learning-databaseonics.uci.edu*, 1994.
- [27] Judea Pearl. *Causality*. Cambridge university press, 2009.
- [28] Walt L Perry. *Predictive policing: The role of crime forecasting in law enforcement operations*. Rand Corporation, 2013.
- [29] Jonas Peters and Peter Bühlmann. Identifiability of gaussian structural equation models with equal error variances. *Biometrika*, 101(1):219–228, 2014.
- [30] Jonas Peters, Dominik Janzing, and Bernhard Schölkopf. *Elements of causal inference: foundations and learning algorithms*. MIT press, 2017.
- [31] Rafael Poyiadzi, Kacper Sokol, Raul Santos-Rodriguez, Tijn De Bie, and Peter Flach. FACE: Feasible and actionable counterfactual explanations. *arXiv preprint arXiv:1909.09369*, 2019.
- [32] Danilo Jimenez Rezende, Shakir Mohamed, and Daan Wierstra. Stochastic backpropagation and approximate inference in deep generative models. In *International Conference on Machine Learning*, pages 1278–1286, 2014.

- [33] Cristóbal Romero and Sebastián Ventura. Preface to the special issue on data mining for personalised educational systems. *User Modeling and User Adapted Interaction*, 21(1):1, 2011.
- [34] Peter Schulam and Suchi Saria. Reliable decision support using counterfactual models. In *Advances in Neural Information Processing Systems*, pages 1697–1708, 2017.
- [35] Shubham Sharma, Jette Henderson, and Joydeep Ghosh. Certifai: A common framework to provide explanations and analyse the fairness and robustness of black-box models. In *Proceedings of the AAAI/ACM Conference on AI, Ethics, and Society*, pages 166–172, 2020.
- [36] Ilya Shpitser and Judea Pearl. Identification of conditional interventional distributions. In *22nd Conference on Uncertainty in Artificial Intelligence, UAI 2006*, pages 437–444, 2006.
- [37] Ilya Shpitser and Judea Pearl. Complete identification methods for the causal hierarchy. *Journal of Machine Learning Research*, 9(Sep):1941–1979, 2008.
- [38] Ricardo Silva and Robert B Gramacy. Gaussian process structural equation models with latent variables. In *Proceedings of the Twenty-Sixth Conference on Uncertainty in Artificial Intelligence*, pages 537–545, 2010.
- [39] Kihyuk Sohn, Honglak Lee, and Xinchun Yan. Learning structured output representation using deep conditional generative models. In *Advances in neural information processing systems*, pages 3483–3491, 2015.
- [40] Jin Tian and Judea Pearl. Causal discovery from changes. In *Proceedings of the Seventeenth conference on Uncertainty in artificial intelligence*, pages 512–521, 2001.
- [41] Jin Tian and Judea Pearl. A general identification condition for causal effects. In *Eighteenth national conference on Artificial intelligence*, pages 567–573, 2002.
- [42] Marc Toussaint. Lecture notes: Gaussian identities. 2011.
- [43] Brian L Trippe and Richard E Turner. Conditional density estimation with bayesian normalising flows. *arXiv preprint arXiv:1802.04908*, 2018.
- [44] Berk Ustun, Alexander Spangher, and Yang Liu. Actionable recourse in linear classification. In *Proceedings of the Conference on Fairness, Accountability, and Transparency*, pages 10–19, 2019.
- [45] Julius von Kügelgen, Paul K Rubenstein, Bernhard Schölkopf, and Adrian Weller. Optimal experimental design via Bayesian optimization: active causal structure learning for Gaussian process networks. *NeurIPS Workshop "Do the right thing": machine learning and causal inference for improved decision making*, 2019.
- [46] Sandra Wachter, Brent Mittelstadt, and Luciano Floridi. Why a right to explanation of automated decision-making does not exist in the general data protection regulation. *International Data Privacy Law*, 7(2): 76–99, 2017.
- [47] Sandra Wachter, Brent Mittelstadt, and Chris Russell. Counterfactual explanations without opening the black box: Automated decisions and the GDPR. *Harv. JL & Tech.*, 31:841, 2017.
- [48] Martin J Wainwright and Michael I Jordan. Graphical models, exponential families, and variational inference. *Foundations and Trends® in Machine Learning*, 1(1-2):1–305, 2008.
- [49] Yixin Wang and David M Blei. The blessings of multiple causes. *Journal of the American Statistical Association*, pages 1–71, 2019.
- [50] Christopher KI Williams and Carl Edward Rasmussen. *Gaussian processes for machine learning*, volume 2. MIT press Cambridge, MA, 2006.
- [51] K Zhang and A Hyvärinen. On the identifiability of the post-nonlinear causal model. In *25th Conference on Uncertainty in Artificial Intelligence (UAI 2009)*, pages 647–655. AUAI Press, 2009.

A Proofs

A.1 Proof of Proposition 2

Proposition 2 (GP-SCM noise posterior). *Let $\{\mathbf{x}^i\}_{i=1}^n$ be an observational sample from (5). For each $r \in [d]$ with non empty parent set $|pa(r)| > 0$, the posterior distribution of the noise vector $\mathbf{u}_r = (u_r^1, \dots, u_r^n)$, conditioned on $\mathbf{x}_r = (x_r^1, \dots, x_r^n)$ and $\mathbf{X}_{pa(r)} = (\mathbf{x}_{pa(r)}^1, \dots, \mathbf{x}_{pa(r)}^n)$, is given by*

$$\mathbf{u}_r | \mathbf{X}_{pa(r)}, \mathbf{x}_r \sim \mathcal{N}(\sigma_r^2(\mathbf{K} + \sigma_r^2 \mathbf{I})^{-1} \mathbf{x}_r, \sigma_r^2(\mathbf{I} - \sigma_r^2(\mathbf{K} + \sigma_r^2 \mathbf{I})^{-1})), \quad (6)$$

where $\mathbf{K} := (k_r(\mathbf{x}_{pa(r)}^i, \mathbf{x}_{pa(r)}^j))_{i,j}$ denotes the Gram matrix.

Proof. First, note that, by definition, \mathbf{u}_r is independent of $\mathbf{f}_r = (f_r(\mathbf{x}_{pa(r)}^1), \dots, f_r(\mathbf{x}_{pa(r)}^n))$ given $\mathbf{X}_{pa(r)}$. Moreover, it follows from the assumed GP-SCM model in (5) and Definition 1, as well as properties of the GP prior, that both are multivariate Gaussian random variables with distributions given by

$$\mathbf{u}_r \sim \mathcal{N}(\mathbf{0}, \sigma_r^2 \mathbf{I}) \quad \text{independently of} \quad \mathbf{X}_{pa(r)}, \quad \text{and} \quad (A.1)$$

$$\mathbf{f}_r | \mathbf{X}_{pa(r)} \sim \mathcal{N}(\mathbf{0}, \mathbf{K}), \quad (A.2)$$

where $\mathbf{0}$ denotes the zero vector (or matrix, see below) and \mathbf{K} is as defined in Proposition 2.

Since independent multivariate Gaussian random variables are jointly multivariate Gaussian, we thus have

$$\begin{pmatrix} \mathbf{u}_r \\ \mathbf{f}_r \end{pmatrix} | \mathbf{X}_{pa(r)} \sim \mathcal{N}(\mathbf{0}, \Sigma), \quad \text{where} \quad \Sigma = \begin{pmatrix} \sigma_r^2 \mathbf{I} & \mathbf{0} \\ \mathbf{0} & \mathbf{K} \end{pmatrix} \quad (A.3)$$

Noting that $\mathbf{x}_r = \mathbf{f}_r + \mathbf{u}_r$ and applying a linear transformation to (A.3), we then obtain

$$\begin{pmatrix} \mathbf{u}_r \\ \mathbf{x}_r \end{pmatrix} | \mathbf{X}_{pa(r)} = \begin{pmatrix} \mathbf{I} & \mathbf{0} \\ \mathbf{I} & \mathbf{I} \end{pmatrix} \begin{pmatrix} \mathbf{u}_r \\ \mathbf{f}_r \end{pmatrix} | \mathbf{X}_{pa(r)} \sim \mathcal{N}(\mathbf{0}, \tilde{\Sigma}), \quad \text{where} \quad \tilde{\Sigma} = \begin{pmatrix} \sigma_r^2 \mathbf{I} & \sigma_r^2 \mathbf{I} \\ \sigma_r^2 \mathbf{I} & \mathbf{K} + \sigma_r^2 \mathbf{I} \end{pmatrix}. \quad (A.4)$$

Conditioning on \mathbf{x}_r and using the conditioning formula [e.g., 42], the result follows:

$$\mathbf{u}_r | \mathbf{X}_{pa(r)}, \mathbf{x}_r \sim \mathcal{N}(\mathbf{0} + \sigma_r^2 \mathbf{I}(\mathbf{K} + \sigma_r^2 \mathbf{I})^{-1}(\mathbf{x}_r - \mathbf{0}), \sigma_r^2 \mathbf{I} - \sigma_r^2 \mathbf{I}(\mathbf{K} + \sigma_r^2 \mathbf{I})^{-1} \sigma_r^2 \mathbf{I}) \quad (A.5)$$

$$\sim \mathcal{N}(\sigma_r^2(\mathbf{K} + \sigma_r^2 \mathbf{I})^{-1} \mathbf{x}_r, \sigma_r^2(\mathbf{I} - \sigma_r^2(\mathbf{K} + \sigma_r^2 \mathbf{I})^{-1})) \quad (A.6)$$

□

A.2 Proof of Proposition 3

Proposition 3 (GP-SCM counterfactual distribution). *Let $\{\mathbf{x}^i\}_{i=1}^n$ be an observational sample from (5). Then, for $r \in [d]$ with $|pa(r)| > 0$, the counterfactual distribution over X_r had $\mathbf{X}_{pa(r)}$ been $\tilde{\mathbf{x}}_{pa(r)}$ (instead of $\mathbf{x}_{pa(r)}^F$) for individual $\mathbf{x}^F \in \{\mathbf{x}^i\}_{i=1}^n$ is given by*

$$X_r(\mathbf{X}_{pa(r)} = \tilde{\mathbf{x}}_{pa(r)}) | \mathbf{x}^F, \{\mathbf{x}^i\}_{i=1}^n \sim \mathcal{N}(\mu_r^F + \tilde{\mathbf{k}}^T(\mathbf{K} + \sigma_r^2 \mathbf{I})^{-1} \mathbf{x}_r, s_r^F + \tilde{k} - \tilde{\mathbf{k}}^T(\mathbf{K} + \sigma_r^2 \mathbf{I})^{-1} \tilde{\mathbf{k}}), \quad (7)$$

where $\tilde{k} := k_r(\tilde{\mathbf{x}}_{pa(r)}, \tilde{\mathbf{x}}_{pa(r)})$, $\tilde{\mathbf{k}} := (k_r(\tilde{\mathbf{x}}_{pa(r)}, \mathbf{x}_{pa(r)}^1), \dots, k_r(\tilde{\mathbf{x}}_{pa(r)}, \mathbf{x}_{pa(r)}^n))$, \mathbf{x}_r and \mathbf{K} as defined in Proposition 2, and μ_r^F and s_r^F are the posterior mean and variance of u_r^F given by (6).

Proof. We follow the three steps of abduction, action, and prediction for computing counterfactual distributions (see §2 for more details). Starting from the factual observation $\mathbf{x}^F \in \{\mathbf{x}^i\}_{i=1}^n$ generated according to

$$x_r^F := f_r(\mathbf{x}_{pa(r)}^F) + u_r^F, \quad (A.7)$$

we first compute the noise posterior (*abduction*). According to Proposition 2 it is given by a marginal of (6), i.e.,

$$u_r^F | \mathbf{X}_{pa(r)}, \mathbf{x}_r \sim \mathcal{N}(\mu_r^F, s_r^F) \quad (A.8)$$

where μ_r^F is given by element F of the mean vector

$$\boldsymbol{\mu}_r = \sigma_r^2(\mathbf{K} + \sigma_r^2 \mathbf{I})^{-1} \mathbf{x}_r \quad (A.9)$$

and s_r^F is given by element (F, F) of the covariance matrix

$$S_r = \sigma_r^2(\mathbf{I} - \sigma_r^2(\mathbf{K} + \sigma_r^2 \mathbf{I})^{-1}) \quad (A.10)$$

of the noise posterior given by (6).

Next, we simulate the hypothetical intervention by updating the structural equation (A.7) (*action step*),

$$x_r^F(\mathbf{X}_{pa(r)} = \tilde{\mathbf{x}}_{pa(r)}) := f_r(\tilde{\mathbf{x}}_{pa(r)}) + u_r^F. \quad (A.11)$$

The GP predictive posterior at the new input $\tilde{\mathbf{x}}_{pa(r)}$ has distribution [see, e.g., 50],

$$f_r(\tilde{\mathbf{x}}_{pa(r)}) | \mathbf{X}_{pa(r)}, \mathbf{x}_r \sim \mathcal{N}(\tilde{\mathbf{k}}^T(\mathbf{K} + \sigma_r^2 \mathbf{I})^{-1} \mathbf{x}_r, \tilde{k} - \tilde{\mathbf{k}}^T(\mathbf{K} + \sigma_r^2 \mathbf{I})^{-1} \tilde{\mathbf{k}}). \quad (A.12)$$

Substituting (A.12) and (A.8) into (A.11) and noting that the sum of two Gaussians is again Gaussian with mean and variance equal to the sums of means and variances of the two individual Gaussians (*prediction step*) completes the proof. □

A.3 Proof of Proposition 4

Proposition 4. *Subject to causal sufficiency, $P_{\mathbf{X}_{d(\mathcal{I})} | do(\mathbf{X}_{\mathcal{I}} = \boldsymbol{\theta}), \mathbf{x}_{nd(\mathcal{I})}^F}$ is observationally identifiable:*

$$p(\mathbf{X}_{d(\mathcal{I})} | do(\mathbf{X}_{\mathcal{I}} = \boldsymbol{\theta}), \mathbf{x}_{nd(\mathcal{I})}^F) = \prod_{r \in d(\mathcal{I})} p(X_r | \mathbf{X}_{pa(r)}) \Big|_{\mathbf{X}_{\mathcal{I}} = \boldsymbol{\theta}, \mathbf{X}_{nd(\mathcal{I})} = \mathbf{x}_{nd(\mathcal{I})}^F}. \quad (\text{A.11})$$

Proof. This is a direct consequence of the properties of causally sufficient (Markovian) causal models, but we include a derivation for completeness. Recall that P factorises over its underlying causal graph \mathcal{G} as follows,

$$p(\mathbf{X}) = \prod_{r \in [d]} p(X_r | \mathbf{X}_{pa(r)}). \quad (\text{A.13})$$

This joint distribution is transformed by the intervention $do(\mathbf{X}_{\mathcal{I}} = \boldsymbol{\theta})$ as follows,

$$P(\mathbf{X}_{-\mathcal{I}}, do(\mathbf{X}_{\mathcal{I}} = \boldsymbol{\theta})) = \delta(\mathbf{X}_{\mathcal{I}} = \boldsymbol{\theta}) \prod_{r \in [d] \setminus \mathcal{I}} P(X_r | \mathbf{X}_{pa(r)}). \quad (\text{A.14})$$

Splitting the non-intervened variables into descendants $d(\mathcal{I})$ and non-descendants $nd(\mathcal{I})$, and conditioning on the intervened variables $do(\mathbf{X}_{\mathcal{I}} = \boldsymbol{\theta})$, we obtain

$$P(\mathbf{X}_{nd(\mathcal{I})}, \mathbf{X}_{d(\mathcal{I})} | do(\mathbf{X}_{\mathcal{I}} = \boldsymbol{\theta})) = \left(\prod_{r \in nd(\mathcal{I}) \cup d(\mathcal{I})} P(X_r | \mathbf{X}_{pa(r)}) \right) \Big|_{\mathbf{X}_{\mathcal{I}} = \boldsymbol{\theta}}. \quad (\text{A.15})$$

As the non-descendants $\mathbf{X}_{nd(\mathcal{I})}$ are, by their very definition, not affected by the intervention, we can write

$$P(\mathbf{X}_{nd(\mathcal{I})}, \mathbf{X}_{d(\mathcal{I})} | do(\mathbf{X}_{\mathcal{I}} = \boldsymbol{\theta})) = \left(\prod_{r \in d(\mathcal{I})} P(X_r | \mathbf{X}_{pa(r)}) \right) \Big|_{\mathbf{X}_{\mathcal{I}} = \boldsymbol{\theta}} \prod_{r \in nd(\mathcal{I})} P(X_r | \mathbf{X}_{pa(r)}).$$

We can thus condition on a particular value of $\mathbf{X}_{nd(\mathcal{I})}$ to obtain

$$P(\mathbf{X}_{d(\mathcal{I})} | do(\mathbf{X}_{\mathcal{I}} = \boldsymbol{\theta}), \mathbf{X}_{nd(\mathcal{I})} = \mathbf{x}_{nd(\mathcal{I})}^F) = \left(\prod_{r \in d(\mathcal{I})} P(X_r | \mathbf{X}_{pa(r)}) \right) \Big|_{\mathbf{X}_{\mathcal{I}} = \boldsymbol{\theta}, \mathbf{X}_{nd(\mathcal{I})} = \mathbf{x}_{nd(\mathcal{I})}^F} \quad (\text{A.16})$$

□

B Further details on CVAE training

To learn the CVAE latent variable models, we perform amortised variational inference with approximate posteriors q parameterised by encoders E_r in the form of neural nets with parameters ϕ_r ,

$$p_{\psi_r}(\mathbf{z}_r | x_r, \mathbf{x}_{pa(r)}) \approx q_{\phi_r}(\mathbf{z}_r | x_r, \mathbf{x}_{pa(r)}) := \mathcal{N}(\hat{\mu}_r, \hat{\sigma}_r^2), \quad (\hat{\mu}_r, \hat{\sigma}_r^2) := E_r(x_r, \mathbf{x}_{pa(r)}; \phi_r). \quad (\text{B.1})$$

The training objective in form of the evidence lower bound (ELBO) given data $\{\mathbf{x}^i\}_{i=1}^n$ is given by

$$\mathcal{L}_r(\psi_r, \phi_r) = \sum_{i=1}^n \mathbb{E}_{q_{\phi_r}(\mathbf{z} | x_r^i, \mathbf{x}_{pa(r)}^i)} \left[\left\| x_r^i - D_r(\mathbf{x}_{pa(r)}^i, \mathbf{z}; \psi_r) \right\|^2 \right] + \beta_r D_{\text{KL}} \left(q_{\phi_r}(\mathbf{z} | x_r^i, \mathbf{x}_{pa(r)}^i) \parallel p(\mathbf{z}) \right) \quad (\text{B.2})$$

We learn both ψ_r and ϕ_r simultaneously via stochastic gradient descend on \mathcal{L}_r , with gradients computed by Monte Carlo sampling from q_{ϕ_r} with reparametrisation. Since the pairs of encoder and decoder parameters (ψ_r, ϕ_r) are independent for different r , this can be done in parallel.

B.1 Hyperparameter selection for CVAE training

A CVAE model was trained for every $\mathbf{X}_r | \mathbf{X}_{pa(r)}$ relation. Generally, hyperparameters were selected by comparing the distribution of real samples from the dataset against reconstructed samples from the trained CVAE obtained by sampling noise from the prior. The selection of hyperparameters was done either manually, or by performing a grid search over various encoder and decoder architectures, latent-space dimensions, and values of the hyperparameters β_r that trade off the MSE and KL terms in the CVAE objective (B.2). For the case of automatic selection, the setup resulting in the smallest maximum mean discrepancy (MMD) statistic [11] between real and reconstructed samples was chosen as hyperparameter configuration. Further details on the search space considered and the selected values are provided in Table 3.

Table 3: Selection of hyperparameters for CVAE training was either performed manually (for Linear SCM, Non-linear ANM, Non-additive SCM) or automatically (for 7-variable semi-synthetic loan approval) by selecting the setting that resulted in the minimum MMD statistic between real and reconstructed samples.

SCM	Conditional	Encoder Arch.	Decoder Arch.	Latent Dim.	λ_{KLD}
Linear SCM	$X_2 X_1,$	$1 \times 32 \times 32 \times 32$	$5 \times 5 \times 1$	1	0.01
	$X_3 X_1, X_2$	$1 \times 32 \times 32 \times 32$	$32 \times 32 \times 32 \times 1$	1	0.01
Non-linear ANM	$X_2 X_1,$	$1 \times 32 \times 32$	$32 \times 32 \times 1$	5	0.01
	$X_3 X_1, X_2$	$1 \times 32 \times 32 \times 32$	$32 \times 32 \times 1$	1	0.01
Non-additive SCM	$X_2 X_1,$	$1 \times 32 \times 32 \times 32$	$32 \times 32 \times 1$	3	0.5
	$X_3 X_1, X_2$	$1 \times 32 \times 32 \times 32$	$5 \times 5 \times 1$	3	0.1
7-variable semi-synthetic loan approval	any		2×1		5, 1, 0.5, 0.1,
		$1 \times 3 \times 3$	$2 \times 2 \times 1$		
		$1 \times 5 \times 5$	$3 \times 3 \times 1$	1,2	0.05, 0.01,
		$1 \times 3 \times 3 \times 3$	$5 \times 5 \times 1$		0.005
			$3 \times 3 \times 3 \times 1$		

C (Non-)identifiability of SCMs under different assumptions

In general form, i.e., without any further assumption on the structural equations \mathbf{S} or noise distribution P_U , SCMs are not identifiable from data alone, meaning that there are multiple different SCMs (possibly with different underlying causal graphs) which imply the same observational distribution [30]. One possible construction relies on the use of the inverse cumulative distribution function (cdf) in combination with uniformly-distributed random variables [9] and is also used in non-identifiability proofs for non-linear independent component analysis (ICA) [13]. Even knowing the causal graph is generally not enough as summarised in the following proposition.

Proposition 5. *Even when the causal graph is known, the conditionals $P(X_r|\mathbf{X}_{pa(r)})$ alone are insufficient to uniquely determine the structural equations $X_r := f_r(\mathbf{X}_{pa(r)}, U_r)$ without further assumptions.*

Proof. This can be shown by using the following argument from [14, Footnote 1] (adapted to our notation):

“let U_r consist of (possibly uncountably many) real-valued random variables $U_r[\mathbf{x}_{pa(r)}]$, one for each value $\mathbf{x}_{pa(r)}$ of the parents $\mathbf{X}_{pa(r)}$. Let $U_r[\mathbf{x}_{pa(r)}]$ be distributed according to $P_{X_r|\mathbf{x}_{pa(r)}}$ and define $f_r(\mathbf{x}_{pa(r)}, U_r) := U_r[\mathbf{x}_{pa(r)}]$. Then $X_r|\mathbf{X}_{pa(r)}$ has distribution $P_{X_r|\mathbf{x}_{pa(r)}}$ ”.

We can now build on this formulation to construct a second SCM with the same observational distribution and causal graph, e.g., by shifting the noise variables and structural equations by some fixed constant C as follows.

For $r \in [d]$, define $Y_r := X_r - C$. Let \tilde{U}_r consist of (possibly uncountably many) real-valued random variables $\tilde{U}_r[\mathbf{x}_{pa(r)}]$, one for each value $\mathbf{x}_{pa(r)}$ of the parents $\mathbf{X}_{pa(r)}$. Let $\tilde{U}_r[\mathbf{x}_{pa(r)}]$ be distributed according to $P_{Y_r|\mathbf{x}_{pa(r)}}$ and define $f_r(\mathbf{x}_{pa(r)}, \tilde{U}_r) := \tilde{U}_r[\mathbf{x}_{pa(r)}] + C$. Then $X_r|\mathbf{X}_{pa(r)}$ also has distribution $P_{X_r|\mathbf{x}_{pa(r)}}$, but for $C \neq 0$ the structural equations and noise distributions are different from the previous construction. \square

In the case of the CVAE-SCM model from (13) the setting is slightly less general than the above, since we additionally assume that: (i) the noise distributions are isotropic multivariate Gaussian distributions of fixed dimension, $\mathbf{z}_r \sim \mathcal{N}_{d_{\mathbf{z}_r}}(\mathbf{0}, \mathbf{I})$; and (ii) the structural equations D_r are from the class of functions that can be expressed as feedforward neural networks of fixed width and depth with learnable parameters ψ_r .

Unfortunately, we are not aware of any identifiability results for this particular setting, and further investigation into this matter is beyond the scope of the current work. It is interesting to note, however, that the CVAE-SCM from (13) can be understood as a non-linear extension of the linear Gaussian model with equal error variances considered by [29], for which identifiability has been shown.

In general, there seem to be very few works addressing identifiability of SCMs in the non-linear case; we refer to [30, §7.1] for an overview of existing results. Of particular interest for our setting is the post-nonlinear model of [51], which refers to the setting in which a non-linearity g is applied on top of an ANM, i.e., $X_r := g_r(f_r(\mathbf{X}_{pa(r)}) + U_r)$, and for which complete conditions on $\{f_r, g_r\}$ have been provided that lead to identifiability. Given the form of the decoders D_r —feedforward neural networks with stacked layers of simple non-linearities applied to linear transformations of the previous layers’ output—it may be possible that the CVAE-SCM from (13) can be interpreted as a nested post-nonlinear model. We consider this an interesting direction, but leave further investigations into this matter for future work.

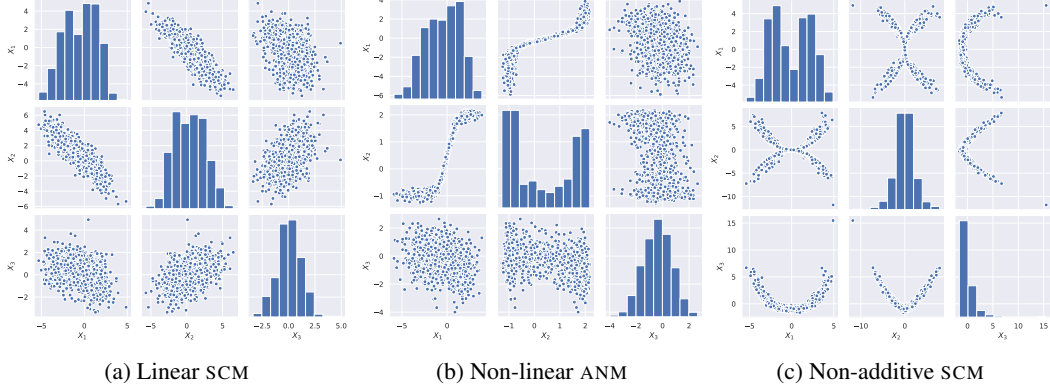


Figure 3: Histograms and scatter plots of pairwise feature relations for the synthetic 3-variable SCMs.

D Experimental details, hyperparameter choices, and specification of SCMs

D.1 Specification of SCMs used in our experiments

The following is a specification of all SCMs used in our experiments on synthetic and semi-synthetic data, both for data generation and to evaluate the validity of recourse actions proposed by the different approaches by computing the corresponding counterfactual in the ground-truth SCMs.

In addition, we also specify the model used to generate training labels. Note, however, that these labels are only used to train a new classifier (e.g., a logistic regression, multi-layer perceptron, or random forest) from scratch: this is the $h(\mathbf{x})$ referred to in the main paper. The label generating process is thus only used for obtaining labels to train a classifier on and is subsequently disregarded in favour of h .

In selecting the structural equations and label generating process, we tried to pick combinations that resulted in roughly centred features, as well as roughly balanced datasets (i.e., with a similar proportion of positive and negative training examples) that are not perfectly linearly-separable (i.e., with some class overlap). Moreover, we tried to select settings that result in a diverse set of intervention targets selected by the oracle for different factual instances, i.e., we try to avoid situations in which the optimal action is to always intervene on the same (set of) variable(s). To induce more interesting behaviour, we sample root nodes from mixtures of Gaussians.

D.1.1 3-variable synthetic SCMs used for Table 1

A visual summary of the 3-variable synthetic SCMs used for Table 1 is provided in Fig. 3.

Linear SCM: The linear 3-variable SCM consists of the following structural equations and noise distributions:

$$X_1 := U_1, \quad U_1 \sim \text{MoG}\left(0.5\mathcal{N}(-2, 1.5) + 0.5\mathcal{N}(1, 1)\right) \quad (\text{D.1})$$

$$X_2 := -X_1 + U_2, \quad U_2 \sim \mathcal{N}(0, 1) \quad (\text{D.2})$$

$$X_3 := 0.05X_1 + 0.25X_2 + U_3, \quad U_3 \sim \mathcal{N}(0, 1) \quad (\text{D.3})$$

Non-linear ANM: The non-linear 3-variable ANM consists of the following structural equations and noise distributions:

$$X_1 := U_1, \quad U_1 \sim \text{MoG}\left(0.5\mathcal{N}(-2, 1.5) + 0.5\mathcal{N}(1, 1)\right) \quad (\text{D.4})$$

$$X_2 := -1 + \frac{3}{1 + e^{-2X_1}} + U_2, \quad U_2 \sim \mathcal{N}(0, 0.1) \quad (\text{D.5})$$

$$X_3 := -0.05X_1 + 0.25X_2^2 + U_3, \quad U_3 \sim \mathcal{N}(0, 1) \quad (\text{D.6})$$

Non-additive SCM: The non-additive 3-variable SCM consists of the following structural equations and noise distributions:

$$X_1 := U_1, \quad U_1 \sim \text{MoG}\left(0.5\mathcal{N}(-2, 1) + 0.5\mathcal{N}(2, 1)\right) \quad (\text{D.7})$$

$$X_2 := 0.25 \text{sgn}(U_2)X_1^2(1 + U_2^2), \quad U_2 \sim \mathcal{N}(0, 0.25) \quad (\text{D.8})$$

$$X_3 := -1 + 0.1(X_1^2 + X_2^2) + U_3, \quad U_3 \sim \mathcal{N}(0, 0.25^2) \quad (\text{D.9})$$

Label generation: For the non-additive 3-variable SCM labels Y were sampled according to

$$Y \sim \text{Bernoulli} \left(\left(1 + e^{5(X_3+0.5)} \right)^{-1} \right) \quad (\text{D.10})$$

For the other two 3-variable SCMs labels Y were sampled according to

$$Y \sim \text{Bernoulli} \left(\left(1 + e^{-2.5\rho^{-1}(X_1+X_2+X_3)} \right)^{-1} \right) \quad (\text{D.11})$$

where ρ is the average of $(X_1 + X_2 + X_3)$ across all training samples.

D.1.2 7-variable semi-synthetic loan approval SCM used for Table 2

For the semi-synthetic dataset, we wanted to capture some relations between the involved variables that seemed somewhat intuitive to us and to some limited extent reflect a loan approval setting in the real-world:

- loan amount and duration being largest for mid-aged people who may want to build a house and start a family, and smaller for younger and older people;
- loan duration increasing with loan amount due to the an upper limit on monthly payments that can be afforded
- savings increasing once income passes a certain (minimal-sustenance) threshold;
- income increasing with age;
- education increasing with age initially before eventually saturating;
- gender differences in income and (access to) education due to existing gender-discrimination and inequality of opportunities in the population;

A visual summary of the 7-variable semi-synthetic loan SCM is shown in Fig. 4.

SCM: The loan approval SCM consists of the following structural equations and noise distributions:

$$G := U_G, \quad U_G \sim \text{Bernoulli}(0.5) \quad (\text{D.12})$$

$$A := -35 + U_A, \quad U_A \sim \text{Gamma}(10, 3.5) \quad (\text{D.13})$$

$$E := -0.5 + \left(1 + e^{-(-1+0.5G+(1+e^{-0.1A})^{-1}+U_E)} \right)^{-1}, \quad U_E \sim \mathcal{N}(0, 0.25) \quad (\text{D.14})$$

$$L := 1 + 0.01(A - 5)(5 - A) + G + U_L, \quad U_L \sim \mathcal{N}(0, 4) \quad (\text{D.15})$$

$$D := -1 + 0.1A + 2G + L + U_D, \quad U_D \sim \mathcal{N}(0, 9) \quad (\text{D.16})$$

$$I := -4 + 0.1(A + 35) + 2G + GE + U_I, \quad U_I \sim \mathcal{N}(0, 4) \quad (\text{D.17})$$

$$S := -4 + 1.5\mathbb{I}_{\{I>0\}}I + U_S, \quad U_S \sim \mathcal{N}(0, 25) \quad (\text{D.18})$$

Note that variables in the above SCM often have a relative meaning in terms of deviation from the mean, e.g., we centre the Gamma-distributed age around its mean of 35, so that A has the meaning of “age-difference from the mean of 35” (and similarly for other variables).

E Additional results

This section presents additional results complementing those from Section 7. Table 4 presents results that mirror those in Table 1, where the brute-force approach discussed at the beginning of §6 is used instead of the gradient-based optimisation. Here, each real-valued feature was discretised into 20 bins within the range of its observed values in the training dataset.

Fig. 5 mirrors the results in Fig. 2c, for which a snapshot ($\gamma_{\text{LCB}} = 2.5$) is also provided in Table 2. Here we show the trade-off between validity and cost by varying the values of γ_{LCB} , using as trained classifiers a non-linear multilayer perceptron (MLP) in (a) and a non-differentiable random forest classifier in (b). Note that optimisation for the latter can only be done with the brute-force approach. All these additional results mostly confirm the insights presented in the main body.

Finally, Table 5 provides a qualitative comparison of the proposed recourse approaches against the oracles and baselines in terms of their selection of intervention targets. We show empirically, on the three synthetic datasets, that CATE approaches have more predictable behaviour, as they are less sensitive to model assumptions, and are thus more preferable for the individual seeking recourse under imperfect causal knowledge.

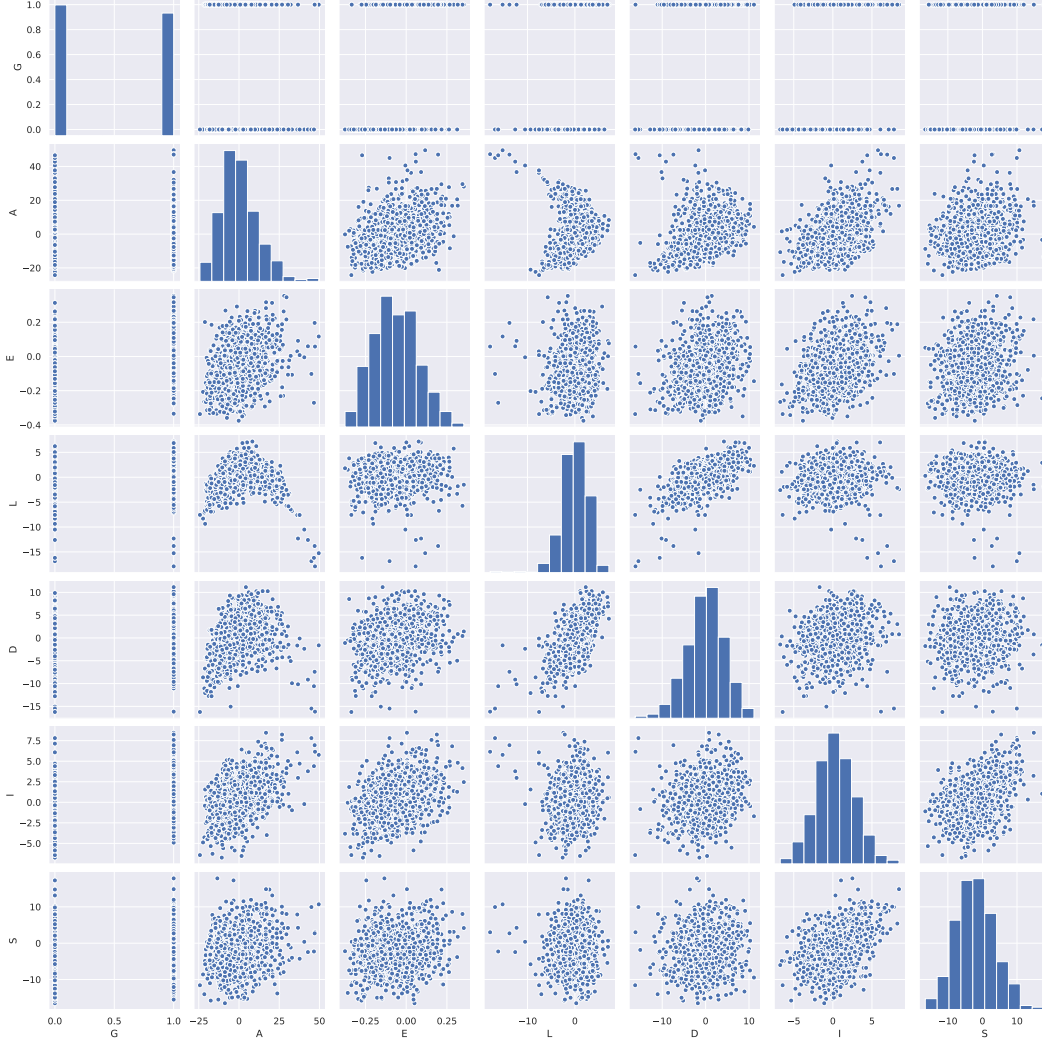


Figure 4: Histograms and scatter plots of pairwise feature relations for the semi-synthetic loan SCM.

Table 4: Experimental results for the brute-force (20-bin discretization) approach on different 3-variable SCMs. We show average performance for $N_{\text{runs}} = 50$, $N_{\text{MC-samples}} = 100$, and $\gamma_{\text{LCB}} = 2$. The relative trends reflect those in Table 1.

Method	LINEAR SCM			NON-LINEAR ANM			NON-ADDITIVE SCM		
	Valid _* (%)	LCB	Cost (%)	Valid _* (%)	LCB	Cost (%)	Valid _* (%)	LCB	Cost (%)
\mathcal{M}_*	100	-	9.7±5.2	100	-	20.9±10.0	100	-	16.2±10.7
\mathcal{M}_{LIN}	100	-	9.9±5.4	58	-	19.6± 8.1	98	-	19.0±17.1
\mathcal{M}_{KR}	100	-	10.1±5.5	96	-	21.0± 9.9	60	-	15.1±11.0
\mathcal{M}_{GP}	100	.57±.05	10.9±5.5	100	.54±.03	21.4± 9.8	90	.80±.12	17.1±12.8
$\mathcal{M}_{\text{CVAE}}$	100	.57±.04	10.9±5.5	90	.54±.02	22.2± 9.6	96	.86±.08	18.8±17.2
CATE _*	92	.55±.09	10.7±5.3	98	.54±.03	22.6± 9.8	76	.81±.12	15.8±10.3
CATE _{GP}	94	.55±.09	10.8±5.3	96	.55±.03	22.8±10.0	94	.84±.09	17.9±14.2
CATE _{CVAE}	96	.57±.07	10.9±5.4	98	.52±.03	22.9± 9.9	96	.82±.14	17.0±12.0

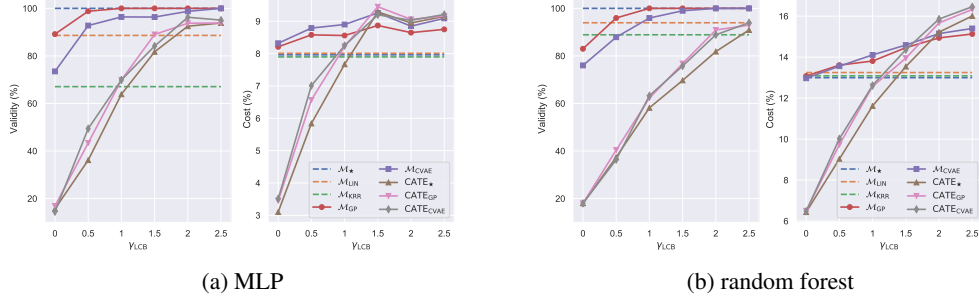


Figure 5: Trade-off between validity and cost which can be controlled via γ_{LCB} for the probabilistic recourse methods. Shown is the same setting as in Fig. 2c using instead a non-linear logistic regression in the form of a multilayer perceptron (MLP; left), and a random forest (right) as classifiers h .

Table 5: Experimental results for the gradient-descent approach on different 3-variable SCMs (top to bottom: linear SCM, non-linear ANM, non-additive SCM). We show average performance for $N_{\text{runs}} = 50$, $N_{\text{MC-samples}} = 100$, and $\gamma_{\text{LCB}} = 2$, and display the number (out of N_{runs}) of performed interventions on all subsets of variables by each recourse type. The two right-most columns display how many of the intervention sets for each recourse type agreed with the suggestions made by the oracle methods, \mathcal{M}_* and CATE_* , respectively. We observe that interventions proposed by the subpopulation-based oracle often differ from the ones proposed at the individual level, which can be visually explained by Fig. 2a. Importantly, we observe general agreement among all CATE approaches in their selection of intervened-upon variables. In contrast, we observe that individual-based methods deviate away from their oracle (i.e., \mathcal{M}_*) in their selection of variables to intervene upon for recourse. This result further suggest that the CATE approaches presented in this work exhibit more predictable behaviour, as they are less sensitive to model assumptions, and are thus more preferable for the individual seeking recourse under imperfect causal knowledge.

Method	SCM			INTERVENTION SET							IDENTICAL INT. SET	
	Valid _* (%)	LCB	Cost (%)	$\{X_1\}$	$\{X_2\}$	$\{X_3\}$	$\{X_1, X_2\}$	$\{X_1, X_3\}$	$\{X_2, X_3\}$	$\{X_1, X_2, X_3\}$	\mathcal{M}_*	CATE_*
\mathcal{M}_*	100	-	7.5±4.1	0	10	0	38	0	0	2	50	13
\mathcal{M}_{LIN}	100	-	7.8±4.2	0	6	0	40	0	1	3	45	15
\mathcal{M}_{KR}	100	-	7.8±4.1	0	6	0	38	0	1	5	43	17
\mathcal{M}_{GP}	100	.54±.03	9.0±4.1	0	3	0	25	0	3	19	24	25
$\mathcal{M}_{\text{CVAE}}$	100	.53±.02	9.0±4.2	0	5	0	26	0	2	17	26	20
CATE_*	96	.54±.04	9.5±4.2	0	0	0	13	0	8	29	13	50
CATE_{GP}	94	.54±.04	9.5±4.2	0	3	0	12	0	7	28	15	40
$\text{CATE}_{\text{CVAE}}$	94	.54±.05	9.6±4.3	0	1	0	9	0	9	31	10	46
<hr/>												
\mathcal{M}_*	100	-	21.2±11.4	20	0	0	0	27	0	3	50	19
\mathcal{M}_{LIN}	52	-	20.1±6.9	3	0	0	0	47	0	0	30	30
\mathcal{M}_{KR}	98	-	21.4±11.4	23	0	0	0	24	0	3	47	19
\mathcal{M}_{GP}	100	.55±.03	23.0±11.7	11	0	0	0	36	0	3	33	24
$\mathcal{M}_{\text{CVAE}}$	96	.54±.04	24.2±10.0	5	0	0	0	43	0	2	24	29
CATE_*	92	.55±.04	24.7±12.2	3	0	0	0	29	0	18	19	50
CATE_{GP}	96	.56±.05	25.3±11.8	1	0	0	1	31	0	17	19	47
$\text{CATE}_{\text{CVAE}}$	98	.53±.03	26.3±11.1	1	0	0	0	30	0	19	19	43
<hr/>												
\mathcal{M}_*	100	-	6.3±3.5	2	0	32	13	3	0	0	50	31
\mathcal{M}_{LIN}	94	-	6.3±3.5	0	1	49	0	0	0	0	31	37
\mathcal{M}_{KR}	90	-	6.2±3.5	8	5	28	9	0	0	0	29	27
\mathcal{M}_{GP}	100	.54±.03	6.2±3.5	3	0	37	10	0	0	0	39	34
$\mathcal{M}_{\text{CVAE}}$	96	.54±.03	6.2±3.5	2	0	47	1	0	0	0	32	38
CATE_*	98	.54±.03	6.2±3.6	10	2	38	0	0	0	0	31	50
CATE_{GP}	92	.53±.03	6.2±3.6	0	2	44	4	0	0	0	31	40
$\text{CATE}_{\text{CVAE}}$	94	.53±.02	6.2±3.6	6	1	43	0	0	0	0	33	45

F Derivation of a Monte-Carlo estimator for the gradient of the variance

We now derive an estimator for the gradient of the square-root of the variance (i.e., standard deviation) of h over the interventional or counterfactual distribution of $\mathbf{X}_{d(I)}$ w.r.t. $\boldsymbol{\theta}$, which appears (multiplied by λ_{LCB}) in the threshold $\text{tresh}(a)$ of the optimisation constraint/regulariser.

First, we use the chain rule of differentiation to write

$$\nabla_{\boldsymbol{\theta}} \sqrt{\mathbb{V}_{\mathbf{X}_{d(I)}} \left[h \left(\mathbf{X}_{d(I)}, \boldsymbol{\theta}, \mathbf{x}_{\text{nd}(I)}^{\text{F}} \right) \right]} = \frac{\nabla_{\boldsymbol{\theta}} \mathbb{V}_{\mathbf{X}_{d(I)}} \left[h \left(\mathbf{X}_{d(I)}, \boldsymbol{\theta}, \mathbf{x}_{\text{nd}(I)}^{\text{F}} \right) \right]}{2 \sqrt{\mathbb{V}_{\mathbf{X}_{d(I)}} \left[h \left(\mathbf{X}_{d(I)}, \boldsymbol{\theta}, \mathbf{x}_{\text{nd}(I)}^{\text{F}} \right) \right]}} \quad (\text{F.1})$$

Next, we write the variance as expectation and—assuming the interventional or counterfactual distribution of $\mathbf{X}_{d(I)}$ admits reparametrisation as is the case for the GP-SCM and CVAE models used in this paper—use the reparametrisation trick to differentiate through the expectation operator as in (15).

$$\nabla_{\boldsymbol{\theta}} \mathbb{V}_{\mathbf{X}_{d(I)}} \left[h \left(\mathbf{X}_{d(I)}, \boldsymbol{\theta}, \mathbf{x}_{\text{nd}(I)}^{\text{F}} \right) \right] \quad (\text{F.2})$$

$$= \nabla_{\boldsymbol{\theta}} \mathbb{E}_{\mathbf{X}_{d(I)}} \left[\left(h \left(\mathbf{X}_{d(I)}, \boldsymbol{\theta}, \mathbf{x}_{\text{nd}(I)}^{\text{F}} \right) - \mathbb{E}_{\mathbf{X}_{d(I)}} \left[h \left(\mathbf{X}_{d(I)}, \boldsymbol{\theta}, \mathbf{x}_{\text{nd}(I)}^{\text{F}} \right) \right] \right)^2 \right] \quad (\text{F.3})$$

$$= \nabla_{\boldsymbol{\theta}} \mathbb{E}_{\mathbf{z} \sim \mathcal{N}(\mathbf{0}, \mathbf{I})} \left[\left(h \left(\mathbf{X}_{d(I)}(\mathbf{z}; \boldsymbol{\theta}), \boldsymbol{\theta}, \mathbf{x}_{\text{nd}(I)}^{\text{F}} \right) - \mathbb{E}_{\mathbf{z}' \sim \mathcal{N}(\mathbf{0}, \mathbf{I})} \left[h \left(\mathbf{x}_{d(I)}(\mathbf{z}'; \boldsymbol{\theta}), \boldsymbol{\theta}, \mathbf{x}_{\text{nd}(I)}^{\text{F}} \right) \right] \right)^2 \right] \quad (\text{F.4})$$

$$= \mathbb{E}_{\mathbf{z} \sim \mathcal{N}(\mathbf{0}, \mathbf{I})} \left[\nabla_{\boldsymbol{\theta}} \left(h \left(\mathbf{X}_{d(I)}(\mathbf{z}; \boldsymbol{\theta}), \boldsymbol{\theta}, \mathbf{x}_{\text{nd}(I)}^{\text{F}} \right) - \mathbb{E}_{\mathbf{z}' \sim \mathcal{N}(\mathbf{0}, \mathbf{I})} \left[h \left(\mathbf{x}_{d(I)}(\mathbf{z}'; \boldsymbol{\theta}), \boldsymbol{\theta}, \mathbf{x}_{\text{nd}(I)}^{\text{F}} \right) \right] \right)^2 \right] \quad (\text{F.5})$$

$$= \mathbb{E}_{\mathbf{z} \sim \mathcal{N}(\mathbf{0}, \mathbf{I})} \left[2 \left(h \left(\mathbf{X}_{d(I)}(\mathbf{z}; \boldsymbol{\theta}), \boldsymbol{\theta}, \mathbf{x}_{\text{nd}(I)}^{\text{F}} \right) - \mathbb{E}_{\mathbf{z}' \sim \mathcal{N}(\mathbf{0}, \mathbf{I})} \left[h \left(\mathbf{x}_{d(I)}(\mathbf{z}'; \boldsymbol{\theta}), \boldsymbol{\theta}, \mathbf{x}_{\text{nd}(I)}^{\text{F}} \right) \right] \right) \right] \quad (\text{F.6})$$

$$\times \left(\nabla_{\boldsymbol{\theta}} h \left(\mathbf{X}_{d(I)}(\mathbf{z}; \boldsymbol{\theta}), \boldsymbol{\theta}, \mathbf{x}_{\text{nd}(I)}^{\text{F}} \right) - \mathbb{E}_{\mathbf{z}' \sim \mathcal{N}(\mathbf{0}, \mathbf{I})} \left[\nabla_{\boldsymbol{\theta}} h \left(\mathbf{x}_{d(I)}(\mathbf{z}'; \boldsymbol{\theta}), \boldsymbol{\theta}, \mathbf{x}_{\text{nd}(I)}^{\text{F}} \right) \right] \right) \quad (\text{F.7})$$

We can now obtain an estimate of the gradient with two independent sets of Monte Carlo samples of $\mathbf{X}_{d(I)}$, drawn via reparametrisation from the interventional or counterfactual distribution,

$$\{\mathbf{x}_{d(I)}^{(m)} := \mathbf{x}_{d(I)}(\mathbf{z}^{(m)}; \boldsymbol{\theta})\}_{m=1}^M, \quad \{\mathbf{x}_{d(I)}^{(m')} := \mathbf{x}_{d(I)}(\mathbf{z}^{(m')}; \boldsymbol{\theta})\}_{m'=1}^{M'} \quad \text{where } \mathbf{z}^{(m)}, \mathbf{z}^{(m')} \stackrel{\text{i.i.d.}}{\sim} \mathcal{N}(\mathbf{0}, \mathbf{I}). \quad (\text{F.8})$$

This yields the following Monte Carlo gradient estimator of the variance:

$$\nabla_{\boldsymbol{\theta}} \mathbb{V}_{\mathbf{X}_{d(I)}} \left[h \left(\mathbf{X}_{d(I)}, \boldsymbol{\theta}, \mathbf{x}_{\text{nd}(I)}^{\text{F}} \right) \right] \approx \frac{1}{M} \sum_{m=1}^M \left[2 \left(h \left(\mathbf{x}_{d(I)}^{(m)}, \boldsymbol{\theta}, \mathbf{x}_{\text{nd}(I)}^{\text{F}} \right) - \frac{1}{M'} \sum_{m'=1}^{M'} h \left(\mathbf{x}_{d(I)}^{(m')}, \boldsymbol{\theta}, \mathbf{x}_{\text{nd}(I)}^{\text{F}} \right) \right) \right] \quad (\text{F.9})$$

$$\times \left(\nabla_{\boldsymbol{\theta}} h \left(\mathbf{x}_{d(I)}^{(m)}, \boldsymbol{\theta}, \mathbf{x}_{\text{nd}(I)}^{\text{F}} \right) - \frac{1}{M'} \sum_{m'=1}^{M'} \nabla_{\boldsymbol{\theta}} h \left(\mathbf{x}_{d(I)}^{(m')}, \boldsymbol{\theta}, \mathbf{x}_{\text{nd}(I)}^{\text{F}} \right) \right) \quad (\text{F.10})$$

Substituting the above expression, together with the following Monte Carlo estimate of the (undifferentiated) variance

$$\mathbb{V}_{\mathbf{X}_{d(I)}} \left[h \left(\mathbf{X}_{d(I)}, \boldsymbol{\theta}, \mathbf{x}_{\text{nd}(I)}^{\text{F}} \right) \right] \approx \frac{1}{M-1} \sum_{m=1}^M \left(h \left(\mathbf{x}_{d(I)}^{(m)}, \boldsymbol{\theta}, \mathbf{x}_{\text{nd}(I)}^{\text{F}} \right) - \frac{1}{M} \sum_{m'=1}^{M'} h \left(\mathbf{x}_{d(I)}^{(m')}, \boldsymbol{\theta}, \mathbf{x}_{\text{nd}(I)}^{\text{F}} \right) \right)^2, \quad (\text{F.11})$$

into (F.1) gives the desired estimate for the gradient of the standard deviation of h .